Porosity and Permeability Prediction through Forward Stratigraphic Simulations Using GPM^{TM} and Petrel^{TM}: Application in Shallow Marine Depositional Settings.

Daniel Otoo and David Hodgetts

Department of Earth and Environmental Sciences, University of Manchester, Manchester, M13 9PL, United Kingdom.

Correspondence to: Daniel Otoo (daniel.otoo@manchester.ac.uk)

Abstract

The forward stratigraphic simulation approach is ~~used in this work~~applied to ~~predict~~forecast porosity and permeability ~~attributes~~trends in the Volve field~~, Norway. This was achieved by using spatial data~~ subsurface model. Variograms and synthetic well logs from the forward stratigraphic model were combined with known data to ~~control the distribution of~~guide porosity and permeability ~~in the 3-D grid.~~distribution. Building a ~~subsurface property~~ reservoir model that fits data at different locations ~~in a hydrocarbon reservoir is a task associated~~ comes with high levels of uncertainty. ~~An~~ Therefore, it is critical to generate an appropriate ~~means to minimise property representation uncertainties is to use geologically realistic sediment distribution and or~~ stratigraphic ~~patterns~~framework to ~~predict~~guide lithofacies ~~units~~ and ~~related~~associated petrophysical ~~properties.~~distribution in a subsurface model. The workflow ~~used are~~adopted is in three parts; first, simulation of twenty scenarios of sediment transportation and deposition using the geological process modeling (GPM^{TM}) software developed by Schlumberger ~~was used to simulate scenarios of sediment deposition in the model area.~~. Secondly, an estimation of the extent and proportion of lithofacies proportions in the stratigraphic model ~~was done~~ using the property calculator tool in ~~the~~ Petrel^{TM} ~~software~~. Finally, porosity and permeability values ~~are~~were assigned to corresponding lithofacies-associations in the forward stratigraphic model to produce a forward stratigraphic-based ~~petrophysical~~porosity and permeability model. Results show a lithofacies distribution ~~that is controlled by~~model, which depends on sediment diffusion rate, sea level variation, flow rate, wave processes, and tectonic events. This observation is consistent with ~~real-world events were~~ the natural occurrence, where variation in sea level ~~changes, volume of~~, sediment ~~input~~supply, and accommodation ~~space~~ control ~~the kind of~~ stratigraphic ~~sequence formed.~~sequences. Validation wells ~~prefixed~~, VP1 and

VP2 located in the original Volve field ~~petrophysical~~ model and the forward stratigraphic-based models show a ~~good match in~~ significant similarity, especially in the porosity ~~and permeability attributes at 5 m vertical sample intervals. By reducing the level of property uncertainty between wells through~~models. These results suggest that forward stratigraphic simulation outputs can be used together with geostatistical modeling~~, an improved porosity and permeability can be achieved for an efficient field development strategy~~ workflows to improve subsurface property representation in reservoir models.

Introduction

The distribution of reservoir properties such as porosity and permeability is a direct function of a complex combination of sedimentary, geochemical, and mechanical processes (Skalinski & Kenter, 2014). The impact of reservoir petrophysics on ~~hydrocarbon field development and depletion~~well planning and production strategies makes it imperative to use reservoir modeling techniques that present realistic property variations ~~in~~via 3-D models (~~e.g.~~ Deutsch and Journel, 1999; Caers and Zhang, 2004; Hu & Chugunova, 2008). Typically, reservoir modeling ~~tasks require~~requires continued property modification until an ~~a~~ appropriate match to ~~known~~ subsurface data ~~is obtained. However, acquisition of~~. Meanwhile, subsurface ~~datasets~~data acquisition is ~~costly~~expensive, thus restricts data collection and accurate subsurface property modeling ~~condition~~. Several studies, ~~e.g.~~ Hodgetts et al. (2004) and Orellana et al. (2014) have demonstrated ~~that~~how stratigraphic patterns, and therefore petrophysical attributes ~~can be fairly well understood from~~ in seismic~~, outcrop~~ data, outcrops, and well logs~~.~~ are applicable in subsurface modeling. However, ~~this notion is limited by~~ the absence of ~~an accurate and reliable~~detailed 3-~~D~~dimensional depositional ~~model~~frameworks to guide ~~the distribution of~~ property ~~variability in reservoir units~~modeling inhibits this strategy (Burges et al. 2008). Reservoir modeling techniques with the capacity to integrate forward stratigraphic simulation outputs with stochastic modeling techniques for subsurface property modeling will improve reservoir heterogeneity characterization, because they more accurately produce geological realism than the other modeling methods (Singh et al. 2013). ~~2013).~~ The use of geostatistical-based methods to represent ~~the~~ spatial variability of reservoir properties ~~have~~has been ~~widely accepted~~ in many exploration and production projects (~~e.g.~~ Kelkar and Godofredo, 2002). In the geostatistical ~~base~~ modeling ~~methods~~method, an alternate numerical 3-D model (~~i.e.~~ realizations) ~~is derived to demonstrate~~shows different ~~scenarios of~~ property distribution scenarios that ~~can be conditioned~~are most likely to match well data (Ringrose & Bentley, 2015). ~~Typically, subsurface modeling practioners are faced with~~However, due to cost reservoir modeling practitioners continue to encounter the challenge of ~~getting a lot of~~obtaining adequate subsurface data to deduce reliable ~~variogram~~

~~models as a result of cost~~variograms for subsurface modeling, therefore introducing a significant level of uncertainty in ~~a~~ reservoir ~~model~~models (Orellena et al. 2014). The advantages of applying geostatistical modeling approaches ~~in populating propoerties in~~ to represent reservoir properties in models ~~is well established (e.g.~~are discussed in studies by Deutsch and Journel~~,~~ (1999~~;~~), Dubrule, (1998~~), but~~). A notable disadvantage is that the geostatistical modeling method tends to confine reservoir property ~~models~~distribution to ~~known~~subsurface data and rarely ~~realize~~produces geological realism to capture sedimentary events that ~~have~~ led to reservoir formation (Hassanpour et al. 2013). In effect, the geostatistical modeling technique ~~is unable to~~does not reproduce ~~a~~ long-range ~~continuity of~~continuous reservoir properties~~ that~~, which are essential for generating realistic reservoir connectivity models (Strebelle & Levy, 2008). ~~Based on lessons from a previous work (e.g. Otoo and Hodgetts, 2019), the~~The forward stratigraphic simulation approach ~~is again~~was applied in this contribution to ~~predict~~forecast lithofacies~~ units~~, porosity, and ~~petrophysical properties~~permeability in a ~~3-D~~reservoir model~~. An important~~, based on lessons from Otoo and Hodgetts (2019). A significant aspect of this work is ~~the use of~~using variogram parameters from forward stratigraphic-based synthetic wells to ~~populate petrophysical properties, especially within inter-well regions of~~simulate porosity and permeability trends in the reservoir ~~under study~~model. Forward stratigraphic modeling involves ~~the uses~~ morphodynamic rules to ~~derive sedimentary depositional patterns to reflect~~replicate 3-dimensional stratigraphic ~~observations~~depositional trends observed in ~~real~~ data~~. The approach is driven by the~~ (e.g. seismic). Forward stratigraphic modeling operates on the guiding principle that multiple sedimentary process-based simulations in a 3-D framework will ~~most likely~~ improve ~~our understanding on spatial variation of~~ facies, ~~as well as~~and therefore petrophysical ~~properties~~property distribution in a geological ~~system~~model.

The ~~sedimentary system, Hugin formation makes up the main~~ geological process modeling GPM™ software (Schlumberger, 2017), which operates on forward stratigraphic simulation principles, replicates a depositional sequence to provide a 3-dimensional framework to predict porosity, permeability in the study area. The reservoir interval ~~in the Volve field. According to studies~~under study is within the Hugin formation. Studies by Varadi et al. (1998); Kieft et al. (2011~~),~~) indicate that the Hugin formation ~~is made~~

~~up~~consists of a complex depositional architecture of waves, ~~tides~~tidal, and ~~riverine riverine~~fluvial processes~~; suggesting~~. This knowledge suggests that a single depositional model will not be adequate to produce a ~~realisite~~realistic lithofacies or petrophysical distributions model of the area. Furthermore, the complicated Syn-depositional rift-related faulting system, significantly ~~influence~~influences the stratigraphic architecture (Milner and Olsen, 1998). ~~The~~ Therefore, the focus ~~of this study~~ here is to produce a depositional sequence, which captures subsurface attributes observed in ~~the shallow marine environment by using a forward stratigraphic modeling approach in the GPM™ (Schlumberger, 2017),~~ seismic and ~~use variogram parameters from the forward model to control porosity and permeability~~ well data to guide property ~~representation in a 3-D model~~modeling.

Study Area

The Volve field (Figure 1), located in Block 15/9 south of the Norwegian North Sea ~~is Jurassic in age (i.e. late Bajocian to Oxfordian) with~~, has the Hugin Formation as the ~~main~~ reservoir ~~unit~~interval from which hydrocarbons are produced (Vollset and Dore, 1984). The Hugin formation, which is Jurassic in age (late Bajocian to Oxfordian), is made up of shallow marine to marginal marine sandstone deposits, coals, and a significant influence of wave events that tend to control lithofacies distribution in the formation (Varadi et al. 1998; and Kieft et al. 2011). ~~Several studies, e.g.~~Studies by Sneider et al. (1995~~),~~) and Husmo et al. (2003) associate sediment deposition ~~in~~into the ~~Hugin system~~study area to ~~a~~ rift-related subsidence and successive flooding during a large transgression of the Viking Graben within the Middle to Late Jurassic period. ~~Previously it was interpreted to comprise~~Also, Cockings et al. (1992), Milner and Olsen (1998) indicate that the Hugin formation comprises of marine shoreface, lagoonal and associated coastal plain, back-stepping delta-plain, and delta front ~~deposits (e.g. Cockings et al. 1992; Milner and Olsen, 1998), but~~. However, recent studies~~, e.g.~~ by Folkestad and Satur~~,~~ (2006) ~~suggest the influence~~also provide evidence of a ~~strong~~high tidal event, which introduces another dimension ~~in property~~that requires attention in any subsurface modeling ~~of~~task in the ~~reservoir~~study area. The thickness of the Hugin formation is estimated ~~to range~~ between 5 m and 200 m, but can be thicker off-structure and non-existent on structurally high segments ~~as a result of~~due to post-depositional erosion (Folkestad and Satur, 2006).

~~Based on studies by Kieft et al. (2011), a~~A summarised sedimentological delineation within the Hugin formation is ~~presented in~~derived based on studies by Kieft et al. (2011). In **Table 1**~~. Lithofacies~~, lithofacies-association codes A, B, C, D, and E ~~used in the classification represents~~represent bay fill units, shoreface sandstone facies, mouth bar units, fluvio-tidal channel fill sediments, and coastal plain facies units, respectively. ~~In addition~~Additionally, a lithofacies association prefixed code F~~ was interpreted to consist~~, which consists of open marine shale units, mudstone~~ with~~. Within it are occasional siltstone beds, parallel laminated soft sediment deformation that locally develop at bed tops. The lateral extent of the code F lithofacies package in the Hugin formation is estimated to be 1.7 km to 37.6 km, but the total thickness ~~have~~of code F lithofacies is not ~~been completely penetrated~~known (Folkestad & Satur, 2006).

Data and Software

This work is based on the description~~,~~ and interpretation of petrophysical datasets in the Volve field by ~~Statoil, now~~ Equinor. Datasets include 3-D seismic ~~data,~~ and a suite of 24 wells that consist of formation pressure data, core data, petrophysical and sedimentological logs. Previous ~~works such as~~ studies by Folkestad & Satur~~,~~ (2006) and Kieft et al~~.~~., (2011) in this reservoir interval show varying grain size, sorting, sedimentary structures, bounding contacts of sediment matrix~~ that play a significant part of the reservoir petrophysics.~~. Grain size, sediment matrix, and the degree of sorting will typically drive the volume of the void created, and therefore the porosity and permeability attributes. Wireline-log attributes such as gamma~~-~~-ray (GR), sonic (DT), density (RHOB), and neutron-porosity (NPHI) ~~were used to~~ distinguish lithofacies units, stratigraphic horizons, and zones that are ~~required to build~~essential for building the 3-D property model~~. Porosity, and permeability models, of the Volve field, were generated~~ in Schlumberger's Petrel™ software. ~~Importantly~~Besides, this ~~work~~study also seeks to produce ~~geologically~~a realistic depositional ~~architecture that is comparable to a real-world~~model like the natural stratigraphic framework in a shallow marine ~~environment. Deriving a representative~~ depositional setting. Therefore, obtaining a 3-~~D~~dimensional stratigraphic model ~~of the reservoir~~that shows a similar stratigraphic sequence observed in the seismic data allows us to deduce ~~geometrical and~~ variogram parameters to serve as input ~~datasets~~ in actual subsurface property modeling.

~~The~~ Twenty forward stratigraphic simulations were produced in the geological process modeling (GPM™) software ~~developed by Schlumberger was used to undertake twenty forward stratigraphic simulation in an attempt to replicate the~~to illustrate depositional processes that resulted in the build-up of the reservoir~~. Simulations were constrained~~ interval under study. By the fourth simulation, there was a development of stratigraphic patterns that shows similar sequences as those observed in seismic, hence the decision to constrain the simulation to twenty scenarios ~~because the desired stratigraphic sequence and associated sediment patterns were achieved at the fourth simulation. Several process modeling software packages exist and have been applied in similar studies; e.g.~~. Delft3D-Flow™; Rijin & Walstra, (2003); DIONISOS™; Burges et al. (2008~~). The geological~~) are examples of subsurface process modeling ~~(GPM™)~~ software ~~was preferred because of the~~ used in similar studies. The availability of the GPM™ software license~~,~~ and ~~also~~ the ~~ease in integrating of its~~capacity to integrate stratigraphic simulation outputs ~~into~~in the property modeling workflow in Petrel™~~.~~ is the reason for using the geological process modeling software in this study.

Methodology

The workflow (Figure 2a) combines the stratigraphic simulation capacity of ~~the~~ GPM™ ~~software~~ in different ~~depositional settings,~~sedimentary processes and the property modeling tools in Petrel™ to predict the distribution of porosity and permeability properties away from ~~well~~known data. ~~Three~~This involves three broad steps ~~have been used here to achieve this goal;~~: (i) forward stratigraphic simulation ~~(FSS)~~ in GPM™ ~~software~~ (2019.1 version), (ii) lithofacies classification using the calculator tool in Petrel™, and (iii) ~~lithofacies,~~ porosity~~,~~ and permeability modeling in Petrel™ (2019.1 version).

~~Process Modeling~~Forward Stratigraphic Simulation in GPM^{TM}

~~The~~ GPM^{TM} is commercial software ~~consist of different~~ developed by Schlumberger to simulate clastic and carbonate sedimentation in a deep or shallow marine environment. GPM^{TM} consists of geological processes ~~designed to~~ such as steady flow, sediment diffusion, tectonics, and sediment accumulation that rely on physical equations and assumptions to replicate ~~sediment~~ the process of sedimentation in a geological basin. A realistic realization of a stratigraphic pattern as observed in seismic or well data provides a 3-dimensional framework to constrain subsurface property representation that conforms with the real-world property distribution trends. In clastic sedimentation, the movement of sediments relies on equations from the original SEDSIM developed in Stanford University (Harbaugh, 1993). Sediment movement, erosion, and deposition ~~in clastic and carbonate environments. Example, the steady flow process is efficient for simulating sediment deposition in fluvial bodies, whilst the unsteady flow process control sediment transportation from the basin slope into deep-water basin setting, largely in the~~is governed by a simplified Navier Stokes equation. “Simplified” because the Navier-Stokes equation in its original form ~~of basinal floor fan units. Previous studies, e.g.~~ define sediment movement in a 3-dimensions differential form, while the flow equation in GPM^{TM} is 2-dimensional with an arbitrary input of flow depth. Kieft et al~~,~~. (2011) ~~identified~~describe the influence of ~~riverine (~~a combination of fluvial~~),~~ and wave processes in the genetic structure of sediments in the Hugin formation. These geological processes ~~could be very~~ are rapid, depending on accommodation ~~space~~ generated ~~as a result of~~ by sea~~-~~-level variation~~,~~ and or sediment composition and flow intensity. ~~Sediment~~The deposition~~,~~ of sediments into a geological basin and its response to post-depositional sedimentary ~~and~~or tectonic processes are significant in the ultimate distribution of subsurface lithofacies ~~units; hence the variation of input parameters to increase our chance attaining outputs that fall within acceptable limits of what may exist in the natural order.~~and petrophysics. Therefore, several input parameters for the forward simulation to attain a stratigraphic output that fits existing knowledge of paleo-sediment transportation and deposition into the study area (see Table 2). The forward simulation ~~generated geologically realistic~~at all stages portrayed geological realism concerning stratigraphic ~~frameworks~~sequence, but it also revealed some limitations, such as instability in the simulator when more than three geological processes ~~and sub-operations run at a time. In view of~~run concurrently. Given this, the diffusion and tectonic processes ~~are~~remained constant ~~features~~ whiles ~~other processes like~~varying the steady flow, unsteady flow, and sediment accumulation~~,~~ ~~compaction were varied.~~ processes in each simulation run.

~~*Parameters*~~Steady & Unsteady Flow Process

The steady flow process in GPM simulates flows that change slowly over a period, or sediment transport scenarios where flow velocity and channel depth do not vary abruptly e.g. rivers at a normal stage, deltas, and sea currents. Considering the influence of fluvial activities during sedimentation in the Hugin formation, it is significant to capture its impact on the resultant simulated output.

The unsteady flow process can simulate periodic flows such as turbidites where the occurrence is not regular, and the velocity of flow changes abruptly over time. The unsteady flow process applies several fluid elements driven by gravity and friction against the hypothetical topographic surface. Otoo and Hodgetts (2019) illustrate how the unsteady process in GPM^{TM} attains realistic distribution of lithofacies units in a turbidite fan system. Although the steady and unsteady flow governing equations distantly rely on the Navier-Stokes equations, the steady flow is quite distinct, as it uses a finite difference numerical method for faster computation and to also illustrate the frequency of flow that is characteristic in channel flow such as rivers. The finite difference method applies an assumption that flow velocity is constant from channel bottom to surface. In contrast, the unsteady flow uses the particle method from SEDSIM3 to solve the sediment concentration in flow and sediment transport capacity (Tetzlaff & Harbaugh 1989). The simplified equation in GPM^{TM} attempts to solve the problem of "shallow-water free-surface flow" over an arbitrary topography surface (Tetzlaff, D. personal communication, February 2021). "Shallow water" indicates the instance where only the vertically-averaged flow velocity and flow depth are applied and kept track of as a function of two horizontal coordinates.

The equation that control steady and unsteady flow is expressed through:

$$\frac{\partial h}{\partial t} + \nabla.hQ = 0 \qquad (1)$$

Where: h is flow depth, t is time, and Q the horizontal flow velocity vector.

$$(\frac{\partial Q}{\partial t} = -(g\nabla)H + \frac{c_2}{\rho}\nabla^2 Q - \frac{c_2 Q/Q/}{h} \qquad (2)$$

Where: $\frac{\partial Q}{\partial t}$ is the Lagrangian derivative of flow relative to time, g is gravity, H is the water surface elevation, c_2 is the fluid friction coefficient, ρ is the water density, c_1 is the water friction coefficient and h is the flow depth.

The Manning's equation is applied to relate flow, slope, flow depth and hydraulic radius channels with a constant cross-section for the steady flow process. Manning's formula states:

$$V = \frac{k}{n} R_h{}^{2/3} S^{1/2} \qquad (3)$$

Where: V is the flow velocity, k is the unit conversion factor, n is the Manning's coefficient which depends on channel rugosity, R_h is the hydraulic radius and S is the slope.

As mentioned earlier, the unsteady flow process uses the particle method equation, which relies on the assumption that erosion and deposition depend on the balance between the flow's transport capacity and the "effective sediment concentration". The equation for multiple-sediment transport in flow is given as follows:

$$A_{em} = \sum_{k_s} \frac{l_{Ks}}{f_{1k_s}} \qquad (4)$$

Where: A_{em} is the effective sediment concentration of mixture, l_{ks} is the sediment concentration of each type, and f_1,k_s is the transportability of each sediment type.

The transport capacity of a sediment type is expressed by equations (5) and (6). Let consider

$$R = (A - A_{em})f_{2,}k_s \qquad (5)$$

Where f_2,k_s is the erosion-deposition rate coefficient for sediment type k_s. For every sediment type ,k_s, the formula for transporting sediment of different grain sizes is given as:

$$(H - Z)\frac{Dl_{Ks}}{Dt} = \begin{cases} R & if\ R > 0\ and\ \tau_0 \geq f_{3,k_s}\ and\ k(x,y,z) = K_s \\ & or\ R < 0\ and\ K_s = 1\ or\ l_{k_s-1} = 0 \\ 0 & otherwise \end{cases} \qquad (6)$$

Where;

H is the free surface elevation to sea level, Z is the topographic elevation for sea level, K_s is the sediment type, $l_{ks,}$ is the volumetric sediment concentration of a specific type (k).

Sediment Diffusion Process

The diffusion process replicates sediment movement from a higher slope (source location) and deposition into a lower elevation of the model area. Sediment diffusion runs on the assumption that sediments are transported downslope at a proportional rate to the topographic gradient, making fine-grained sediments easily transportable than coarse-grained sediments. Sediment diffusion depends on three parameters: (i) sediment grain size and turbulence in the flow, (ii) diffusion curve that serves as a unitless multiplier in the algorithm and, (iii) diffusion coefficient. The diffusion coefficient depends, among other variables on the type of sediment and "energy" of the depositional environment. In this contribution, the highest depth-dependent diffusion coefficient occurs near sea level, where the "energy" is highest over a geological time (Dashtgard et al. 2007).

In GPM™, sediment diffusion is calculated using a simplified expression:

$$\frac{\partial z}{\partial t} = D_i \nabla^2 z + S_n \qquad (7)$$

where **z** is topographic elevation, D_i is the diffusion coefficient, **t** for time, and $\nabla^2 z$ is the laplacian of z, and S_n is the sediment source term.

Sediment diffusion (D_i) is estimated by assuming that the grain size for each sediment component (coarse sand, fine sand, silt, and clay) are known. Also an assumption that these sediment types have a uniform diameter (D) in the flow mix (Dade & Friend 1998; and Zhong 2011). In that case, external fore (F_e), which consist of drag, lift, virtual mass, and Basset history force is given as:

$$F_e = \alpha_e M_e + \alpha_e \Phi_D . \frac{U_{fi} - U_{ei}}{T_p} \quad (8)$$

M_e is the resultant force of other forces with the exception of drag force, T_p stokes relation time, expressed as: $T_p = \rho_\rho D^2/(18\rho_f V_f)$, with ρ_f and V_f as density and viscosity of fluid respectively. Φ_D is a coefficient that accounts for the non-linear dependence of drag force on grain slip Reynolds number (R_p).

$$\Phi_D = \frac{\mathrm{Rp}}{24} C_D \quad (9)$$, with C_D sediment grain coefficient.

With the flow component in place, the diffusion coefficient (D_i) is deduced from the Einstein equation. Using an assumption that the diffusion coefficient decreases with increasing grain size and rise in temperature, and that the coefficient f is known, the expression for D_i is:

$$D_i = \frac{K_B . T}{f} \quad (10)$$

Meanwhile, f is a function of the dimension of the spherical particle involved at a particular time (t). In accounting for f, the equation for D_i changes into:

$$D_i = \frac{K_B . T}{6.\pi.\eta_o.r} \quad (11)$$

Sediment Accumulation

The sediment accumulation process in GPM is designed to generate an arbitrary amount of sediment representing the artificial vertical thickness of a lithology as interpreted in a well or outcrop data (Tetzlaff, D., personal communication, February 2021). The areal input rates for each sediment type (coarse-grained, fine-grained sediments) use the value of the map surface at each cell in the model and multiply it by a value from a unitless curve at each time step in the simulation to estimate the thickness of sediments accumulated or eroded from a cell in the model. Sediment accumulation in the GPM software requires other processes such as steady flow and diffusion to account for sediment transport (sediment entering or leaving a cell) before a deposition/year (mm/yr) function to artificially produce the height of sediment deposited per cell. The accumulation of sediments in GPM is expressed as:

$$A_T = \sum_{S=1}^{n} [(M_{v1} * S_{c1}), \_ \_ n] \quad (12)$$

Where;

A_T is the total sediment accumulated in a cell over a period, S is the sediment type, M_v is the map value of sediment in each cell, and S_C is the sediment supply curve as a function of topographic elevation.

Boundary Conditions for Forward Stratigraphic Simulation

~~A realistic~~Realistic reproduction of stratigraphic patterns in the ~~study~~model area ~~require~~requires input parameters (~~also known as~~ initial conditions~~). These include: a hypothetical~~), such as paleo-topography, sea~~-~~-level curves, sediment source location, and distribution curve, tectonic ~~events (i.e.~~ event maps (subsidence and uplift), and sediment mix velocity. The application of these input parameters in ~~the~~ GPM™ ~~simulator,~~ and their ~~influence~~impact on the resultant stratigraphic framework ~~are explained~~is below.

Hypothetical Paleo-Surface: The hypothetical paleo-~~surface, on which~~topographic for the stratigraphic simulation ~~commences was inferred~~is from the seismic ~~section. Here, we assume~~data (Figure 3), using the assumption that the present day stratigraphic surface~~, also referred to as the~~ (paleo shoreline in Figure ~~3a~~4a) occurred as a result of basin filling ~~through different~~over geological ~~periods~~time. Since the ~~hypothetical topography generated~~surface obtained from the seismic section have undergone various phases of subsidence and uplifts ~~over time,~~, it is significant to note that the paleo topographic surface used in this work does not ~~present~~represent an accurate description of the basin at the period of sediment deposition~~. To mitigate this~~; thus presenting another level of uncertainty~~, 5~~ in the simulation. To derive an appropriate paleo-topographic for this task, five paleo topographic surfaces (TPr) were generated~~ stochastically~~, by adding or subtracting elevations from the inferred paleo topographic surface ~~or base topography~~ (see Figure 4g) using the equation:

$$TPr = Sbs + EM \quad (13)$$

where, Sbs is the base surface scenario (in this instance, scenario 6), and EM an elevation below and above the base surface. ~~In this work,~~

The paleo-topographic surface in scenario 3 (figure ~~3d) was used as the paleo-topographic surface,~~4d) is selected because it produced a stratigraphic sequences that fit the ~~conceptual knowledge of~~ depositional ~~framework as observed in~~patterns interpreted from the seismic section (Figure 5d).

Sediment Source Location: Based on regional well correlations in ~~previous studies (e.g.~~ Kieft et al. 2011~~),~~, and seismic interpretation of the basin structure ~~interpreted from seismic data~~, the sediment entry point ~~for this task was~~is placed in the north-eastern section of the hypothetical paleo-topography~~. Since the~~ surface. The exact sediment entry point ~~is uncertain, multiple~~into this basin is unknown, so three entry points were placed at a 4 ~~m~~km radius around the primary location ~~in~~ (Figure 3c~~), in order~~) to capture possible sediment source locations~~.~~ in the model area. The source position is ~~characterised by~~ a positive ~~integers (i.e.~~ integer (values greater than zero) to enable ~~fluid flow~~sediment movement to other parts of the ~~simulation~~topographic surface.

Sea Level: ~~Primarily, the~~The sea~~-~~ level ~~variation relative to elevation was inferred~~curve is deduced from published studies and facies description in shallow marine depositional environments (e.g. Winterer and Bosellini, 1981). ~~Considering the limitations in the software, we assumed a~~To sea level ~~of~~was constrained 30 m for short simulation runs~~, e.g.~~ (5000 to 20000 years~~ to attain stability in the simulator and~~), but varied ~~it accordingly~~ with the increasing duration of the simulation~~.~~ (see Table 2). The peak sea-level in the simulation ~~represents~~depicts the maximum flooding surface~~,~~ (Figure 5d), and therefore ~~an~~the inferred sequence boundary in the geological process model.

Diffusion and Tectonic Event Rates: The sediment mix proportion~~ and diffusion rate for the simulation were stochastically inferred from previous studies (e.g. Burges et al., 2008), primarily to attain a prograding and or aggrading clinoforms features that are noticeable in real world geological outcrops. The subsidence and uplift rates were kept constant in most part of the model . The~~ , diffusion rate, and tectonic event functions are ~~inferred~~ from ~~published works; e.g.~~studies such as Walter, (1978~~;~~), Winterer and Bosellini, ~~1981, and~~(1981), and Burges et al., (2008). The diffusion and tectonic event rates were increased or reduced to produce a stratigraphic model that fit our knowledge of ~~the~~ basin evolution~~. The simulation parameters applied (**Table 2**) were generated randomly using the~~ in the study area. For example, in scenario 1 (Figure 6a), the early stages of clinoform development show resemblance to interpreted trends in the seismic section (**Figure 3b**). The process commenced with a diffusion coefficient of 8 m2/a, but it varied at each scenario to obtain diffusion coefficients to improve the model. Excluding the initial ~~run (**Figure 6a**) as a guide. The guiding principle for parameter selection is their capacity to produce stratigraphic outputs that depict different depositional scenarios in the shallow marine setting. A sudden change in subsidence rate tends to constrain coarse to medium sediments at proximal distance to source location than in scenarios where the rate of subsidence was made gradual.~~

~~The influence of~~topography (Figure 4d), input parameters in ~~the simulation is evident whenever~~geological processes such as wave events, steady/unsteady flow, diffusion, and tectonic events used curve functions to provide variations in the simulation.

The sensitivity of input parameters in the forward stratigraphic simulation is notable when there is a ~~slight~~ change of value in sediment diffusion, and tectonic rates or dimension of the hypothetical ~~topographic surfaces.~~topography. For example, a change in sediment source position ~~has a strong impact on~~affects the extent and depth ~~to which~~of sediments ~~are deposited~~deposition in the ~~basin~~simulation. Shifting the source point to the mid-section of the topography (the mid-point of the topography in a basin-ward direction) resulted in the accumulation of distal elements ~~that are~~ identical to turbidite lobe systems. This output is consistent with morphodynamic experiments ~~(e.g.~~by de Leeuw et al~~.,~~. (2016~~)~~), where ~~abrupt~~sediment discharge ~~of sediments~~ from the basin slope leads to the build-up of basin floor fan units. ~~Stratigraphic patterns generated using different input parameters provides 3-D perspective into subsurface property variations under alternating initial conditions.~~

Property Classification in Stratigraphic Model

In our opinion, the most appropriate output is the stratigraphic model in ~~this work is~~ **Figure 5d**. This point of view is because, ~~it produced a stratigraphic sequence that mimics~~ compared to the depositional ~~sequence~~description in ~~the shallow marine depositional environment under study. The stratigraphic model was converted into a 3-D format, 20 m x 20 m x 2 m grid cells in order to be used in~~studies such as

Folkestad and Satur (2006); Kieft et al. (2011), and the ~~property modeling tool in Petrel™. Lithofacies, porosity, and permeability properties are characterized in the stratigraphic using a rule based approach (**Table 3**).~~seismic interpretation presents a similar stratigraphic sequence. Sediment distribution in each time step of the simulation ~~were~~was stacked into a single zone framework to attain a simplified model. This ~~was done with the assumption~~strategy assumes that sedimentary processes that lead to the final build-up of genetic related units within zones of the ~~forward stratigraphic architecture~~ model will not vary significantly over the simulation period. ~~Property classification in the~~The stratigraphic model (**Figure 5d**) was ~~achieved with~~converted into a 3-D format (20 m x 20 m x 2 m grid cells) for the property ~~calculator tool~~modeling in Petrel™.

Facies, porosity, and permeability representation in ~~Petrel.~~the stratigraphic model was done via a rule based approach in Petrel™ (see **Table 3**). The classification is driven by depositional depth, geologic flow velocity, and sediment distribution patterns as indicated in **Figure 7**. Lithofacies representation in the stratigraphic model ~~was based~~relied on the sediment grain size pattern~~,~~ and proximity to sediment source. For example, shoreface lithofacies units ~~were characterized using~~ are medium-to-coarse grained sediments ~~to that are~~, which accumulate at a proximal distance to the sediment source~~, whiles~~. In contrast, mudstone units are ~~constrained to the distal parts of the stratigraphic model, where~~ confined to fine~~-~~-grained sediments ~~accumulate at~~in the ~~end~~distal section of the simulation domain.

~~Porosity~~Using knowledge from published studies by Kieft et al. (2011) and wireline-log attributes such as gamma ray, neutron, sonic, and density logs, porosity and permeability variations ~~were~~in the stratigraphic model are estimated ~~from published wireline-log attributes (e.g. Kieft et al., 2011), which is outlined in~~ (Table 1~~. Based~~). In previous studies on ~~petrophysical report of~~ the Sleipner Øst, and Volve field (~~Statoil~~Equinor, 2006~~), a deduction was made to the effect that high net-to-gross zones will be associated with~~; Kieft et al. 2011), shoreface deposits make up the best ~~quality~~ reservoir units~~; classified as shoreface lithofacies~~, whiles lagoonal deposits formed the worst reservoir units~~, whilst low net-to-gross zones were interpreted to be connected with high proportions of shale or~~. With this guide, shoreface sandstone units and mudstone ~~deposits.~~/shale units in the forward stratigraphic model are best and worst reservoir units respectively. The porosity and ~~184~~ permeability values in Table 4 ~~were derived~~are from equations in Statoil's petrophysical report of the Volve ~~185~~ field (~~Statoil~~Equinor, 2016):

$$\varnothing_{er} = \varnothing_D + \alpha \cancel{x}. (NPHI - \varnothing_D) + \beta \cancel{;} \qquad (14)$$

where $\varnothing_{er}$ is the estimated porosity range, $\varnothing_D$ is density porosity, α and β are regression constants; ranging between -0.02 – 0.01 and 0.28 – 0.4 respectively, *NPHI* is neutron porosity. In instances where NPHI values for lithofacies units is not available from the published references, an average of 0.25 was used.

$$KLOGH_{er} = 10^{(2 + 8 * PHIF - 5 * VSH\cancel{;})} \qquad (15)$$

where $KLOGH_{er}$ is the estimated permeability range, *VSH* is the volume of clay/shale in the lithofacies unit, and *PHIF*, the fractured porosity. The *VSH* range between 0.01 – 0.12 for the shoreface units, and 0.78 – 0.88 for lagoonal deposits.

Property Modeling in Petrel™

The workflow (**Figure 2b**) used for subsurface property ~~(e.g. lithofacies, and petrophysical)~~ modeling in Petrel™ is ~~extended~~applied to represent lithofacies, porosity, and permeability properties in the ~~forward~~ stratigraphic model. These processes ~~include~~involve:

~~1.~~(1) Structure ~~modelling~~modeling: identified faults within the study area are ~~modelled~~modeled together with interpreted surfaces from seismic and well ~~data~~correlation to generate the main structural framework, within which the ~~entire~~ property model ~~will be~~is built. ~~The procedures involve modification of~~Here, fault pillars and connecting fault bodies are linked to ~~one another to attain~~obtain the kind of fault framework interpreted from the seismic ~~and core~~ data.

~~(1)~~(2) Pillar gridding: building a "grid skeleton" ~~that is~~ made up of a top, middle and base architectures. Typically, ~~there are~~ pillars ~~which~~ join corresponding corners of every grid cell of the adjacent grid~~, forming~~ to form the foundation ~~of~~for each cell within the model~~; hence its nomenclature as a corner point gridding.~~. The prominent orientation of faults (I-direction) within the model ~~is~~area was in an N-S and NE-SW direction, so the "I-direction" was set ~~the major~~

~~direction along which grid cells align.~~to NNE-SSW to capture the general structural description of the area.

~~(2)~~(3) Horizons, Zones, and Vertical Layering: stratigraphic horizons and subdivisions (zones) ~~delineates~~delineate the geological formation's boundaries. As stratigraphic horizons are ~~inserted~~introduced into the model grid, the surfaces are trimmed iteratively and modified along faults to correspond with displacements across multiple faults. Vertical layering ~~on the other hand~~ ~~defines~~shows the thicknesses and orientation between the layers of the model. ~~In order~~Layers refers to ~~honour~~significant changes in particle size or sediment composition in a geological formation. Using a vertical layering scheme makes it possible to honor the fault framework, pillar grid, and horizons ~~that have been derived. Cell thicknesses are defined~~. A constant cell thickness of 1 m is used in the model to control the vertical scale~~, in which subsurface properties such as~~ of lithofacies, porosity, and permeability ~~attributes are modelled~~modeling.

~~(3)~~(4) Upscaling~~; which~~: involves ~~averaging~~the substitution of ~~finer~~smaller grid cells ~~in order~~with coarser grid cells. Here, log data is transformed from 1-dimensional to ~~assign property values~~a 3-dimensional framework to ~~the cells and~~ evaluate which discrete value suits ~~each~~selected data point~~. It also encompasses~~ in the ~~generation~~model. One advantage of ~~coarser grids (i.e. lower resolution grids) in~~ the ~~geological model, in order~~upscaling procedure is to make ~~simulation~~the modeling process faster.

Porosity and Permeability Modeling

The Volve field porosity and permeability model ~~that was built by~~from Equinor ~~for their operations~~ ~~was~~are adopted as the base (reference) model. The model, which ~~cover an area of~~covers 17.9 km^2 was generated with the reservoir management software (RMS), developed by Irap and Roxar (Emerson^{TM}). The ~~original~~ petrophysical model has a grid dimension of 108 m x 100 m x 63 m~~,~~ and was compressed by 75.27% of cell size~~.~~ from an approximated cell size of 143 m x 133 m x 84 m. To achieve a comparable model resolution ~~to~~as the ~~original~~Volve field porosity and permeability model, the forward stratigraphic output ~~was~~, which had an initial resolution of 90 m x 78 m x 45 m, is upscaled to a ~~cell size~~grid of 107 m x 99 m x 63 m. ~~Two~~Variograms being a critical aspect of this work, we submit two options ~~were explored with respect to the use of~~ to extrapolate variogram parameters ~~derived~~ from the forward ~~model~~stratigraphic-based ~~synthetic wells.~~porosity and permeability models. In Option 1 ~~was to assign,~~ the porosity and permeability values were assigned to the synthetic lithofacies wells ~~to correspond to~~ that correlate with known facies-~~associations as indicated~~association in the study area (see **Table 4**~~.~~).

The ~~synthetic~~pseudo wells ~~with~~comprising porosity and permeability ~~data~~ are ~~placed~~situated in-between ~~actual~~ well ~~(known data)~~ locations to guide porosity and permeability ~~property distribution~~simulation in the model. For option 2, the best-fit forward stratigraphic model ~~was populated with~~changes by assigning porosity~~,~~ and permeability ~~attributes.~~attribute using the general stratigraphic orientation captured in the seismic data (NE-SW; 240º). Porosity and permeability pseudo (synthetic) logs ~~are~~were then extracted from the forward stratigraphic output to build the porosity and permeability models (**Figure 8**). ~~The second option provided a broader framework for evaluating the reliability of forward stratigraphic simulation on property~~ Porosity modeling is through normal distribution ~~in areas of sparse data. Taking into account~~, whiles the permeability models were produced using a log-normal distribution and the ~~possibility~~corresponding porosity property for collocated co-kriging.

Considering that vertical trends in options 1 and 2 will ~~most likely produce a~~be similar ~~trend in~~within a sampled interval, ~~it is our opinion that~~ option 2 ~~will provide~~presented a viable 3-D representation of property variations in the major and minor directions of the forward stratigraphic model. Ten synthetic wells~~,~~ (SW), ranging between 80 m and ~~a~~ 120 ~~were~~ m in total depth (TD), are positioned in the forward model to capture the vertical distribution of porosity-permeability at different sections of the forward stratigraphic ~~model. Typically, sediment distribution, and associated petrophysical attributes are directly related to depth within the geological model; thus aiding in the analysis of the most likely proportions of subsurface properties that match with observations in known well data~~-based models.

The ~~forward-based~~ synthetic wells (**Figure 9 c**) with porosity and permeability ~~logs~~data were upscaled ~~to populated~~, and distributed into the original structural model using the sequential Gaussian simulation method. The synthetic wells derived from the stratigraphic model served as an additional control for porosity and permeability modeling in the Volve field. Because the variogram-based modeling approach is efficient in subsurface data conditioning, this idea presents an opportunity to get more wells at no additional cost to control porosity and permeability distribution. The variogram model (**Figure 10**~~),~~) of dominant lithofacies units in the ~~formation~~stratigraphic model served as a guide in ~~the estimation of~~estimating variogram parameters ~~from the forward model. A~~for porosity and permeability modeling. The variogram has major and minor range of 1400 m and 400 m respectively, and an average sill value of 0.75~~ derived from forward stratigraphic-based synthetic wells were used to populate porosity and permeability properties in the model. Porosity models were derived with a normal distribution, whilst the permeability models were produced using a log-normal distribution and the corresponding porosity property for collocated co-kriging. Out~~. Six out of fifty model realizations~~, six realizations~~ that ~~showed~~show some similarity to the original ~~petrophysical~~porosity and permeability model ~~are presented~~formed the basis of our analysis (**Figure 11**). The selection of six realizations was on a visual and statistical comparison of zones in the original Volve field model and the stratigraphic-based porosity/permeability model. The statistical approach involved summary statistics from the reference model and the stratigraphic-based porosity/permeability model. In contrast, the visual evaluation compared the geological realism of forward stratigraphic-based realizations to the base model.

Results

The stratigraphic model in stage 4 (**Figure 5d iv**) shows the final geometry after 700,~~-~~000 years of simulation time. ~~Initial~~ The initial stratigraphic simulation produced a progradation sequence with foreset-like features (**Figure 5d i**~~). A~~) and a sequence boundary, which ~~indicates the highest sea level in the model~~ separates the initial simulated output from the next prograding phase (**Figure 5d ii**). ~~Initiation of an aggradation~~An aggradational stacking pattern ~~starts,~~commences and becomes prominent in stage 3 (**Figure 5d iii**). ~~This is~~ These aggradational sequences observed in the forward stratigraphic model are consistent with ~~real-world scenario~~ natural events where sediment supply matchup with accommodation

~~space generated as a result of the relative constant sea~~ due to sea-level rise within a ~~period. The diffusion process in GPM™ was used to define the stratigraphic architecture before introducing additional~~ geological ~~processes such as steady flow, unsteady flow, wave events to capture the range of possible depositional styles that have been discussed in published literature (e.g. Folkestad & Satur, 2006; Kieft et al., 2011).~~period (Muto and Steel, 2000; Neal and Abreu, 2009).

~~The impact~~Impact of the forward stratigraphic simulation on porosity and permeability representation in the reservoir model is ~~evaluated~~evident by comparing its outcomes to the ~~original~~Volve field porosity and permeability models ~~of the Volve~~by using two synthetic well ~~prefixed~~ (VP1 and VP2~~. The synthetic well are~~); sampled at a 5 m ~~intervals vertically to estimate the distribution of porosity and permeability attributes along wells. Considering that the original porosity and permeability model~~ vertical interval. Taking into account the fact that the Volve field petrophysical model (**Figure 11a**) ~~have undergone~~went through various phases of history matching to ~~enable~~obtain a model to improve well planning and ~~guide~~ production strategies ~~in the Volve field~~, it is reasonable to assume that porosity and permeability distribution in the ~~Volve field~~ petrophysical model will be geologically realistic and less uncertain. ~~A~~This view formed the basis for using the porosity and permeability models developed by Equinor as a reference for comparing outputs in the stratigraphic model. **Table 5a** shows an almost good match in porosity ~~was observed in validation wells that penetrate the model realizations;~~at different intervals in the forward stratigraphic-based models (i.e. R14, R20, R26, R36, R45, and R49 ~~(**Table 5a**). The vertical distribution (**Figure 12**)~~). An analysis, of ~~porosity~~ the well logs in ~~selected~~the model ~~realizations~~area, shows that a ~~modal distribution range (i.e.~~large proportion of reservoir porosity is between 0.18 – 0.24~~) that~~. Also, the analysis of the forward stratigraphic-based porosity model is consistent with the ~~original model. The forward stratigraphic-based model have been derived~~porosity range in the Volve field model (see Figure 12).

A notable limitation with ~~an~~ this approach is the assumption that variogram parameters~~,~~ and stratigraphic inclination within zones ~~will remain~~remained constant~~. However,~~ throughout the simulation. The difference in permeability attributes between the original ~~petrophysical~~permeability model ~~takes into~~

~~account~~and the forward stratigraphic-based type is the application of other measured ~~attributes, which could be the main driver of the differences in permeability estimates noted in~~ parameters in the original model (**Table 5b**~~.~~). Typically, a petrophysical model like the Sleipner Øst and Volve field model will ~~take into account~~ factor in other ~~sources of data~~datasets such as special core analysis (SCAL) and ~~other petrophysical evaluations~~level of cementation, which enhances reservoir petrophysics assessment. Bearing in mind that the forward stratigraphic model did not involve some of this additional information from the reservoir~~ section, so~~, it is ~~reasonably reliable~~practicable to suggest that results obtained in the forward stratigraphic-based porosity and permeability models have ~~been~~ adequately conditioned to known subsurface data.

Discussion

~~The results~~Results show the influence of sediment transport rate~~,~~ (or ~~in this example,~~ diffusion rate~~,~~), initial basin topography, and ~~proximity to~~ sediment source location on the stratigraphic simulation in ~~the~~in GPM^{TM}~~ software. Notably, variations in~~. Compared to studies such as Muto & Steel (2000) and Neal & Abreu (2009), we observed that a variation in sea~~-~~-level controls the volume of sediment that ~~could be~~is retained or transported further into the basin~~;~~, therefore controlling the ~~kind of~~resultant stratigraphic sequences~~ that are generated.~~. In ~~a~~ related work~~ by~~, Burges et al. (2008~~), it was established~~) suggest that~~; for example,~~ a sediment-wedge topset width ~~was~~connects directly ~~linked~~ to the initial bathymetry, in which the sediment-wedge structure ~~was formed, as well as~~develops, and the correlation between sediment supply and accommodation rate. This opinion is in line with observations in this ~~work~~study, where the initial sediment deposit ~~control~~controls the geometry of subsequent ~~phase~~phases of depositions~~.~~ ~~Since the~~ in the hypothetical basin. The uncertainty of initial conditions used in this work led to the generation of ~~this basin is uncertain,~~ multiple ~~simulation~~ forward stratigraphic scenarios ~~were carried out~~ to account for the range of bathymetries that may have influenced ~~the build-up of sediments~~sediment transportation to form the ~~Hugin formation.~~ present-day reservoir units in the Volve field.

The simulation produced well~~-~~-defined ~~clinoform~~sloping depositional surfaces in a stratigraphic architecture (clinoforms) and sequence boundaries that depict ~~the pattern observed~~ patterns seen in the seismic data. ~~As indicated in other studies, (e.g.~~ In their work, Allen and Posamentier~~,~~ (1993~~;~~); Ghandour and Haredy~~,~~ (2019) explained the importance of sequence stratigraphy ~~is vital~~ in ~~the~~lithofacies characterization ~~of lithofacies in shallow marine settings; hence, the forward stratigraphic simulation outputs provide a good framework to better understand the variation of lithofacies units in the reservoir through a 3-D perspective. A~~ , and therefore petrophysical property distribution in sedimentary systems. Also, sediment deposition into a geological basin in the natural order is controlled by mechanical and geochemical processes that modify petrophysical attributes (Warrlich et al. 2010); therefore, using different geological processes and initial conditions to generate depositional scenarios in 3-dimension provides a framework to analyse property variations in a hydrocarbon reservoir. The approach produces a porosity-permeability model ~~that match~~ comparable to the original petrophysical model ~~was produced~~ using synthetic porosity and permeability logs from the forward stratigraphic model as input datasets ~~in the sequential Gaussian simulation algorithm.~~. As mentioned ~~previously~~, this ~~exercise~~work did not ~~take into account~~include variations in the layering scheme that develops in different zones of the stratigraphic model. ~~we concede that~~Under this circumstance, there is a possibility to overestimate and or underestimate porosity and permeability ~~properties as observed~~property in some sampled intervals ~~of~~in the validation wells. ~~In view of~~Therefore, we suggest that the forward stratigraphic simulation outputs such as the example presented in this~~, it is our suggestion that forward stratigraphic simulation outputs should be applied~~ contribution serve as additional data to understand sediment distribution patterns~~,~~ and associated vertical and horizontal petrophysical trends in the depositional environment ~~than using its outputs as an~~, and not as absolute conditioning data in subsurface property modeling.

The assumptions made ~~in~~concerning the type of geological processes~~,~~ and input parameters ~~to use~~ in the stratigraphic simulation ~~significantly~~certainly differ from what ~~may have~~ existed during ~~the period of~~ sediment deposition. ~~Applying~~So, applying stratigraphic models that fit a basin~~-~~-scale description to a relatively smaller scale reservoir ~~context~~ presents another ~~degree~~level of uncertainty in the approach ~~used~~

~~here. For example, in their study,~~. This finding agrees with Burges et al., (2008~~) shows~~), where they indicate that the diffusion geological process simulation fits the description of large~~-~~-scale sediment transportation~~; suggesting~~. This view further buttresses the point that ~~an extrapolation of its outputs~~integrating forward stratigraphic simulation into a well-scale framework ~~could produce results~~has a high chance of producing outcomes that deviate from the real~~-~~-world ~~architecture. In reality, sediment deposition into a geological basin is also controlled by mechanical and geochemical processes, which tend to modify a formations petrophysical attributes (Warrlich et al. 2010), hence, the application of different geological processes and initial conditions to produce different depositional scenarios, from which a best fits stratigraphic framework of the reservoir can be selected. Many forward stratigraphic-based~~ subsurface ~~modeling studies (e.g.~~description. In line with observations in Bertoncello et al. (2013~~;~~); Aas et al. (2014~~;~~); and Huang et al. (2015~~), have identified and discussed some~~) in relations to limitations ~~with the technique. Considering that similar challenges were faced in this work, caution must be taken in using the outputs from~~in the forward stratigraphic ~~simulations in real~~simulation method, it is advisable to use its outputs cautiously in reservoir modeling; as ~~this~~such outputs from forward stratigraphic models could lead to an increase ~~uncertainty~~ in ~~the~~property representation ~~of lithofacies and petrophysical properties.~~ bias in a model.

The correlation between reservoir lithofacies and petrophysics, and its prediction through reservoir models, have been extensively examined in ~~previous~~several studies~~, e.g.~~ (Falivene et al~~. (~~., 2006~~)~~; Hu and Chugunova, ~~(~~2008~~), but~~). Meanwhile, the~~ difference in~~ predicted ~~and~~outputs most often do not depict the actual reservoir character ~~is less understood. This in large part is~~ due to the absence of a realistic 3-D stratigraphic framework to guide reservoir property representation in ~~geocellular~~geological models. ~~It is our opinion that~~The forward stratigraphic modeling ~~methods provide~~method, notwithstanding its limitations, provides reservoir modeling practitioners ~~a better~~an platform to generate ~~appropriate 3-D lithofacies models to improve petrophysical property prediction in a reservoir, but its outputs should be used cautiously and together with verifiable~~ subsurface ~~patterns from seismic and well data~~models that reflect the natural variation of reservoir properties.

Conclusion

In this paper, ~~spatial data~~ variogram parameters from a forward stratigraphic simulation ~~is~~are combined with subsurface data ~~from the Volve field, Norway~~ to constrain porosity and permeability distribution in ~~inter-well regions of~~ the Volve field model~~area. As~~. The caution~~,~~ for subsurface modeling practitioners is that the ~~forward~~ stratigraphic simulation scenarios presented in this contribution do not ~~ultimately~~ prove that spatial and geometrical data derived from forward stratigraphic ~~modeling can be used as~~models are absolute input parameters for a real-world reservoir modeling task. Uncertainties in the choice of ~~initial condition~~boundary conditions and processes for the stratigraphic simulation led the variation of input parameters ~~in order~~ to attain a depositional architecture that is geologically realistic and comparable to the stratigraphic correlation suggested in some published studies of the study area. ~~Significantly, the good~~The match in porosity obtained ~~from~~by comparing validation wells in the original and stratigraphic-based petrophysical model~~, leads us to the suggestion~~ indicates that ~~an integration of~~combining variogram parameters from ~~real~~ well data and forward stratigraphic simulation outputs will improve property prediction in inter-well zones. ~~In addition, this~~This suggestion supports the idea that more conditioning data (well data) will increase the chance of producing realistic property distribution in the model area. This work also made some key findings:

1. For ~~a~~ specific ~~application of forward~~ stratigraphic ~~modeling~~simulation in GPM™ and a range of model parameters, ~~the process of~~ sediment transportation and deposition is ~~influenced by~~ based on diffusion rate~~,~~ and proximity to sediment source. This opinion is consistent with several published works on sequence ~~stacking~~stratigraphy and or system tracts in shallow marine settings~~, but~~. However, further work with different stratigraphic modeling simulators could ~~be useful in mitigating~~mitigate some of the challenges faced in this work.
2. ~~A geologically viable 3-D~~A lithofacies distribution ~~in the shallow marine Hugin formation~~that is consistent with previous studies was ~~achieved, which~~produced in the stratigraphic model. This position is evident in scenarios where sediment distribution vertically matches with lithofacies variation in a sampled interval in an actual well log.

Geologically feasible stratigraphic patterns generated in the forward stratigraphic model provide additional confidence in the representation of lithofacies, and therefore porosity and permeability property variations in the depositional setting under study. ~~By reducing the level of property uncertainty between wells, a reliable reservoir model can be generated to guide field planning and development in the hydrocarbon exploration and production industry.~~ The resultant forward stratigraphic-based porosity and permeability model suggests that forward stratigraphic simulation outputs can be integrated into classical modeling workflows to improve subsurface property modeling and well planning strategies.

~~Future studies will focus on using an artificial neural network approach to classify lithofacies associations in the forward stratigraphic model in an attempt to reduce uncertainties that arise from cognitive or sampling biases in the calculator (or rule-based) approach for estimating lithofacies proportion in a forward stratigraphic model. In addition, efforts will be made in a future contribution to compare the stratigraphic property distribution with ones that are generated more classical methods such as sequential indicator simulation (SIS), and object-based modeling.~~

Data and Code Availability

The datasets ~~used in~~for this work ~~was obtained~~are from Equinor on their operations in Volve field ~~operations~~, Norway. ~~This~~The data include~~:~~ 24 suits of well logs, and 3-D reservoir models in Eclipse and RMS formats. The data, models (eclipse and RMS formats), and the rule-based calculation script to generate lithofacies and porosity/permeability proportions are archived on Zenodo as Otoo & Hodgetts, (2020).

GPM™ Software

The ~~version~~ (2019.1) version of GPM™ software was used in completing this work after an initial 2018.1 version. Available on: https://www.software.slb.com/products/gpm. The software license and code used in the GPM™ cannot be provided, because Schlumberger does not allow the code for its software to be shared in publications.

Model Availability in Petrel™

The work started in Petrel™ software (2017.1~~)~~), but it was ~~initially used for the task, but~~ completed with Petrel™ software (2019.1~~);~~). The software is available on: https://www.software.slb.com/products/petrel. The software ~~run~~runs on a ~~windows~~Windows PC with the following specifications: Processor; Intel Xeon CPU E5-1620 v3 @3.5GHz 4 cores-8 threads, Memory; 64 GB RAM. The computer should be high end, because a lot of processing time is required ~~to execute a~~for the task. The forward stratigraphic models are ~~achieved~~ in Zenodo as Otoo & Hodgetts, (2020).

Author Contribution

Daniel Otoo designed the model workflow, conducted the simulation using the GPM™ software, and evaluated the results. David Hodgetts converted the Volve field data into Petrel compactible format for easy integration with outputs from the forward stratigraphic simulation.

Acknowledgement

Thanks to Equinor for making available the Volve field dataset. Also, thanks to Schlumberger for providing us with the GPM™ software license. A special thanks to ~~Schlumberger for providing the~~

~~software, and~~ Mostfa Legri (Schlumberger) for his technical support in the use of GPM^{TM}. Finally, to the Ghana National Petroleum Corporation (GNPC) for sponsoring this research.

References

Aas, T., Basani, R., Howell, J. & Hansen, E.: Forward modeling as a method for predicting the distribution of deep-marine sands: an example from the Peira Cava sub-basin. The geologic society, 387(1), 247-269, doi:10.1144/SP387.9, 2014.

Allen, G. P. and Posamentier, H. W.: Sequence stratigraphy and facies model of an incised valley fill; the Gironde Estuary, France. Journal of Sedimentary Research; 63 (3), 378–391, doi:/10.1306/D4267B09-2B26-11D7-8648000102C1865D, 1993.

Bajpai, V.N., Saha Soy, T.K., Tandon, S.K.: Subsurface sediment accumulation patterns and their relationships with tectonic lineaments in the semi-arid Luni river basin, Rajasthan, Western India. Journal of Arid Environments, 48(4); 603-621, 2001.

Bertoncello, A., Sun, T., Li, H., Mariethoz, G., & Caers, J.: Conditioning Surface-Based Geological Models to Well and Thickness Data. International Association of Mathematical Geoscience, 45, 873-893, doi: 10.1007/s11004-013-9455-4, 2013.

Burges, P.M., Steel, R.J., & Granjeon, D.: Stratigraphic Forward Modeling of Basin-Margin Clinoform Systems: Implications for Controls on Topset and Shelf Width and Timing of Formation of Shelf-Edge deltas. Recent advances in models of siliciclastic shallow-marine stratigraphy. SEPM (Society for Sedimentary Geology) Special Publication, vol. 90, SEPM (Society for Sedimentary Geology), 35-45, 2008.

Caers, J., & Zhang, T.: Multiple-point geostatistics: a quantitative vehicle for integrating geologic analogs into multiple reservoir models, in Grammer, G. M., Harris, P. M., and Eberli, G. P., eds., Integration of outcrop and modern analogs in reservoir modeling. Am. Assoc. Petrol. Geol. Memoir, 384–394, 2004.

Cheng, F., Garzione, C., Jolivet, M., Guo, Z., Zhang, D., & Zhang, C.: A New Sediment Accumulation Model of Cenozoic Depositional Ages From the Qaidam Basin, Tibetan Plateau. Journal of Geophysical Research; Earth Surface. 123, 3101-3121, 2018

Cockings, J.H., Kessler, L.G., Mazza, T.A., & Riley, L.A.: Bathonian to mid-Oxfordian Sequence Stratigraphy of the South Viking Graben, North Sea. Geological Society, London, Special publications, 67, 65–105, doi:10.1144/GSL.SP.1992.067.01.04, 1992.

Dade, W.B. & Friend, P.F.: Grain Size, Sediment Transport Regime, and Channel Slope in Alluvial Rivers. The Journal of Geology, 106(6), 661-676, 1998.

Dashtgard, S.E., White, R.O., Butler, K.E., Gingras, M.: Effects of relative sea level change on the depositional character of an embayed beach, Bay of Fundy, Canada. Marine Geology, 239(3), 143-161, 2007.

Deutsch, C. & Journel, A.: GSLIB. Geostatistical software library and user's guide. Geological magazine, 136(1), 83-108, doi:10.2307/1270548, 1999.

De Leeuw, J., Eggenhuisen, J.T., & Cartigny, M.J.B.: Morphodynamics of submarine channel inception revealed by new experimental approach. Nature Communication, 7, 10886, 2016.

Dubrule, O.: Geostatistics in Petroleum Geology. American Association of Petroleum Geologist, 38, 27-101, doi:10.1306/CE3823, 1998.

Falivene, O., Arbues, P., Gardiner, A., & Pickup, G.E.: Best practice stochastic facies modeling from a channel-fill turbidite sandstone analog (the Quarry outcrop, Eocene Ainsa basin, northeast Spain. American Association of Petroleum Geologist, 90(7), 1003-1029, doi:10.1306/02070605112, 2006.

Folkestad, A., & Satur, N.: Regressive and transgressive cycles in a rift-basin: Depositional model and sedimentary partitioning of the Middle Jurassic Hugin Formation, Southern Viking Graben, North Sea. Sedimentary Geology. 207, 1-21, doi:10.1016/j.sedgeo.2008.03.006, 2008.

Ghandour, I.M. and Haredy, R.A.: Facies Analysis and Sequence Stratigraphy of Al-Kharrar Lagoon Coastal Sediments, Rabigh Area, Saudi Arabia: Impact of Sea-Level and Climate Changes on Coastal Evolution. Arabian Journal for Science and Engineering, 44(1), 505-520, 2019.

Harbaugh, J.W.: Simulating Sedimentary Basins: An Overview of the SEDSIM Model and its Relevance to Sequence Stratigraphy. Geoinformatics, 4(3), 123-126, 1993.

Hassanpour, M., Pyrcz, M. & Deutsch, C.: Improved geostatistical models of inclined heterolithic strata for McMurray formation, Canada. AAPG Bulletin, 97(7), 1209-1224, doi:10.1306/01021312054, 2013.

Hodgetts, D.D., Drinkwater, N.D., Hodgson, J., Kavanagh, J., Flint, S.S., Keogh, K.J. and Howell, J.A.: Three-dimensional geological models from outcrop data using digital data collection techniques: an example from the Tanqua Karoo depocenter, South Africa. Geological Society, London, v. 171 (4), 57–75, doi:10.1144/GSL.SP.2004.239.01.05, 2004.

Hu, L.Y., and Chugunova, T.: Multiple-point geostatistics for modeling subsurface heterogeneity: A comprehensive review. Water Resource Research, 44 (11), 1-14, doi:10.1029/2008WR006993, 2008.

Huang, X., Griffiths, C. & Liu, J.: Recent development in stratigraphic forward modeling and its application in petroleum exploration. Australian journal of Earth science, 62(8), 903-919, doi:10.1080/081200991125389, 2015.

Husmo, T. & Hamar, G.P. & Høiland, O. & Johannessen, E.P. & Rømuld, A. & Spencer, A.M. & Titterton, Rosemary.: Lower and Middle Jurassic. In: The Millennium Atlas: Petroleum Geology of the Central and Northern North Sea, 129-155, 2003.

Kelkar, M., & Perez, G.: Applied Geostatistics for Reservoir Characterization. Society of Petroleum Engineers. https://www.academia.edu/36293900/Applied Geostatistics for Reservoir characterization. Accessed 10 September, 2019, 2002.

Kieft, R.L., Jackson, C.A.-L., Hampson, G.J., and Larsen, E.: Sedimentology and sequence stratigraphy of the Hugin Formation, Quadrant 15, Norwegian sector, South Viking Graben. Geology Society, London, Petroleum Geology Conference Series, 7, 157-176, doi:10.1144/0070157, 2011.

Milner, P.S., and Olsen, T.: Predicted distribution of the Hugin Formation reservoir interval in the Sleipner Øst field, South Viking Graben; the testing of a three-dimensional sequence stratigraphic model. In: Gradstein, F.M., Sandvik, K.O., Milton, N.J. (Eds.), Sequence Stratigraphy; Concepts and Applications. Special Publication, Vol 8. Norwegian Petroleum Society, 337-354, 1998.

Muto, T., and Steel, R.J.: The accommodation concept in sequence stratigraphy: Some dimensional problems and possible redefinition. Geology, 130(1), 1-10, 2000.

Neal, J., and Abreu, V.: Sequence stratigraphy hierarchy and the accommodation succession method. Geology, 37(9), 779-782, 2009.

Otoo, D., and Hodgetts, D.: Geological Process Simulation in 3-D Lithofacies Modeling: Application in a Basin Floor Fan Setting. Bulletin of Canadian Petroleum Geology, 67(4), 255-272, 2019.

Otoo, D. & Hodgetts, D. Data citation for a forward stratigraphic-based porosity and permeability model developed for the Volve field, Norway. Dataset. Zenodo. http://doi.org/10.5281/zenodo.3855293, 2020.

Orellana, N. Cavero, J. Yemez, I. Singh, V. and Sotomayor, J.: Influence of variograms in 3D reservoir-modeling outcomes: An example. The leading edge, 33(8), 890-902, doi:10.1190/tle33080890.1, 2014.

Patruno, S., and Hansen, W.H.: Clinoforms and clinoform systems: Review and dynamic classification scheme for shorelines, subaqueous deltas, shelf edges and continental margins. Earth-Science Reviews, 185, 202-233, 2018.

Ravasi, M., Vasconcelos, I., Curtis, A. and Kristi, A.: Vector-acoustic reverse time migration of Volve ocean-bottom cable data set without up/down decomposed wavefields. Geophysics 80 (4): 137-150, doi:10.1190/geo2014-0554.1, 2015.

Ringrose., P. & Bentley., M.: Reservoir model design: A practioner's guide. First edition ed. New York: Springer business media B.V. 20-150, 2015.

Rijn, L.C., Walstra, D.J.R., Grasmeijer, B., Sutherland, J., Pan, S., & Sierra, J.P.: The predictability of cross-shore bed evolution of sandy beaches at the time scale of storms and seasons using process-based profile models. Coastal engineering, 47(3), 295-327, doi:10.1016/S0378-3839(02)00120-5, 2003.

Schlumberger™ Softwares.: Geological Process Modeling, Petrel™ version 2019.1, Schlumberger, Norway. URL: https://www.sdc.oilfield.slb.com/SIS/downloads.aspx, 2019.

Sclater, J.G. & Christie, P.A.F.: Continental stretching: An explanation of the Post-Mid-Cretaceous subsidence of the central North Sea Basin. Journal of Geophysical Research, Solid Earth; 85(7), 3711-3739, 1980.

Singh, V., & Yemez, I., & Sotomayor de la Serna, J.: Integrated 3D reservoir interpretation and modeling: Lessons learned and proposed solutions. The Leading Edge. 32(11), 1340-1353, doi:10.1190/tle32111340.1, 2013.

Skalinski, M., & Kenter, J.: Carbonate petrophysical rock typing: Integrating geological attributes and petrophysical properties while linking with dynamic behaviour. Geological Society, London, Special Publications. 406 (1), 229-259, 2014.

Sneider, J.S., de Clarens, P., and Vail, P.R.: Sequence stratigraphy of the Middle and Upper Jurassic, Viking Graben, North Sea. In: Steel, R.J., Felt, V.L., Johannessen, E.P., Mathieu, C. (Eds.), Sequence Stratigraphy on the Northwest European Margin. Special Publication, vol. 5. Norwegian Petroleum Society, 167–198, doi:10.1016/S0928-8937(06)80068-8, 1995.

Statoil, "Sleipner Øst, Volve Model, Hugin and Skagerrak Formation Petrophysical Evaluation, 2006", Stavanger, Norway. Accessed on: April, 27, 2019. Online: https://www.equinor.com/volve-field-data-village-download.

Strebelle, S., & Levy, M.: Using multiple-point statistics to build geologically realistic reservoir models: the MPS/FDM workflow. Geological Society London, special publication, 309, 67-74, doi:10.1144/SP309.5, 2008.

Tetzlaff, D.M. & Harbaugh, J.W.: Simulating Clastic Sedimentation. New York: Van Nostrand Reinhold, 1989.

Otoo, D. 2021: Conversation with Daniel Tetzlaff, 4 February.

Varadi, M., Antonsen, P., Eien, M., & Hager, K.: Jurasic genetic sequence stratigraphy of the Norwegian block 15/5 area, South Viking Graben. In: Gradstein, F. M., Sandvik, K.O., & Milton, N.J., (eds) Sequence Stratigraphy – Concepts and Applications. Norwegian Petroleum Society, Trondheim, special publication, 373-401, 1998.

Vollset, J. and Dore, A.G.: A revised Triassic and Jurassic lithostratigraphic nomenclature for the Norwegian North Sea. NPD Bulletin Oljedirektoratet, 3, 53, 1984.

Walter C. P.: Relationship between eustacy and stratigraphic sequences of passive margins. GSA Bulletin; 89 (9), 1389–1403, 1978.

Winterer, L. W., Bosellini, A.: Subsidence and Sedimentation on Jurassic Passive Continental Margin, Southern Alps, Italy. AAPG Bulletin; 65 (3), 394–421, doi: 10.1306/2F9197E2-16CE-11D7-8645000102C1865D, 1981.

Warrlich, G., Hillgartner, H., Rameil, N., Gittins, J., Mahruqi, I., Johnson, T., Alexander, D., Wassing, B., Steenwinkel, M., & Droste, H.: Reservoir characterisation of data-poor fields with regional analogues: a case study from the Lower Shuaiba in the Sultanate of Oman, p. 577, 2010.

Zhong, D.: Transport Equation for Suspended Sediments Based on Two-Fluid Model of Solid/Liquid Two-Phase Flows. Journal of Hydraulic Engineering; 137(5), 530-542, doi: 10.1061/(ASCE)HY.1943-7900.0000331, 2011.

List of Figures

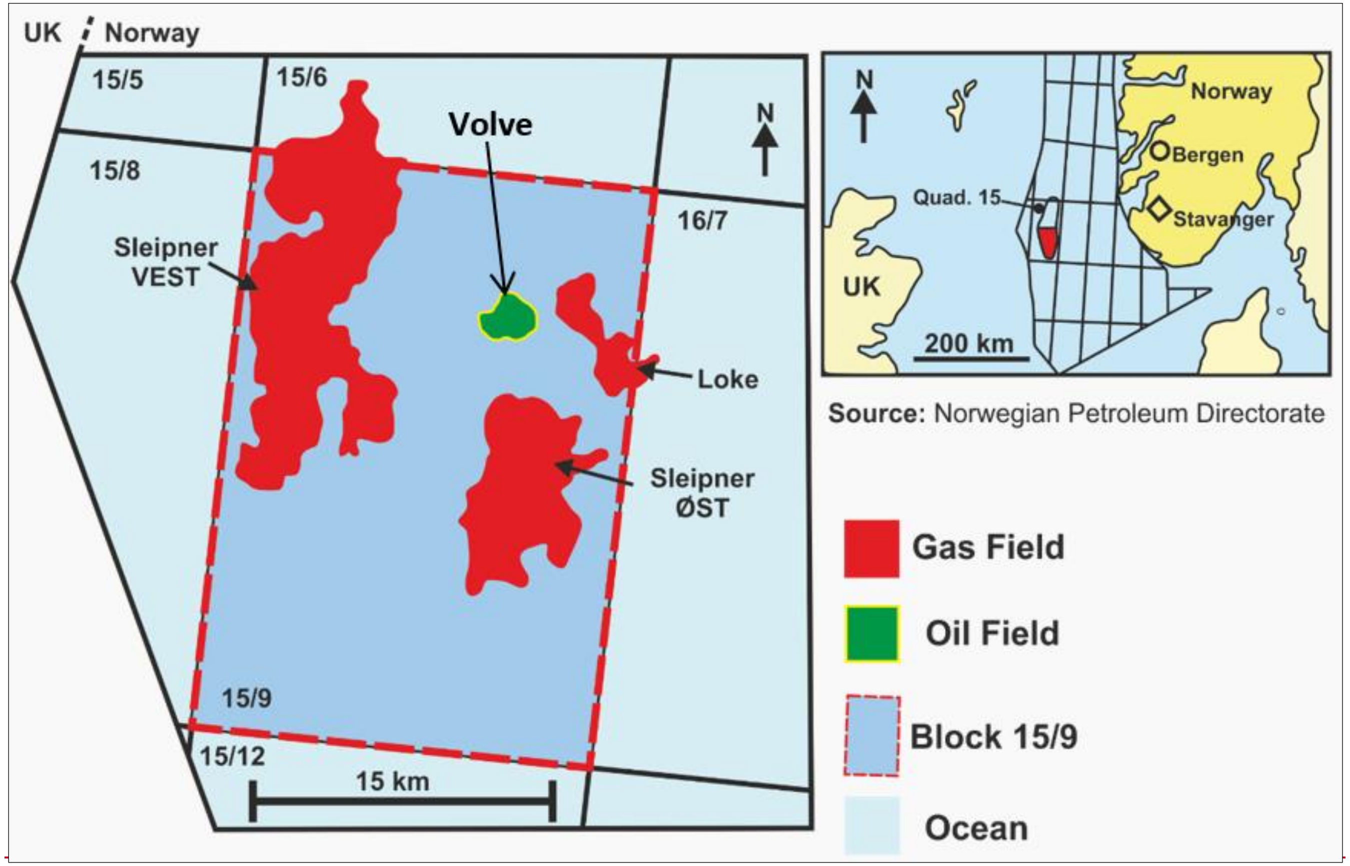

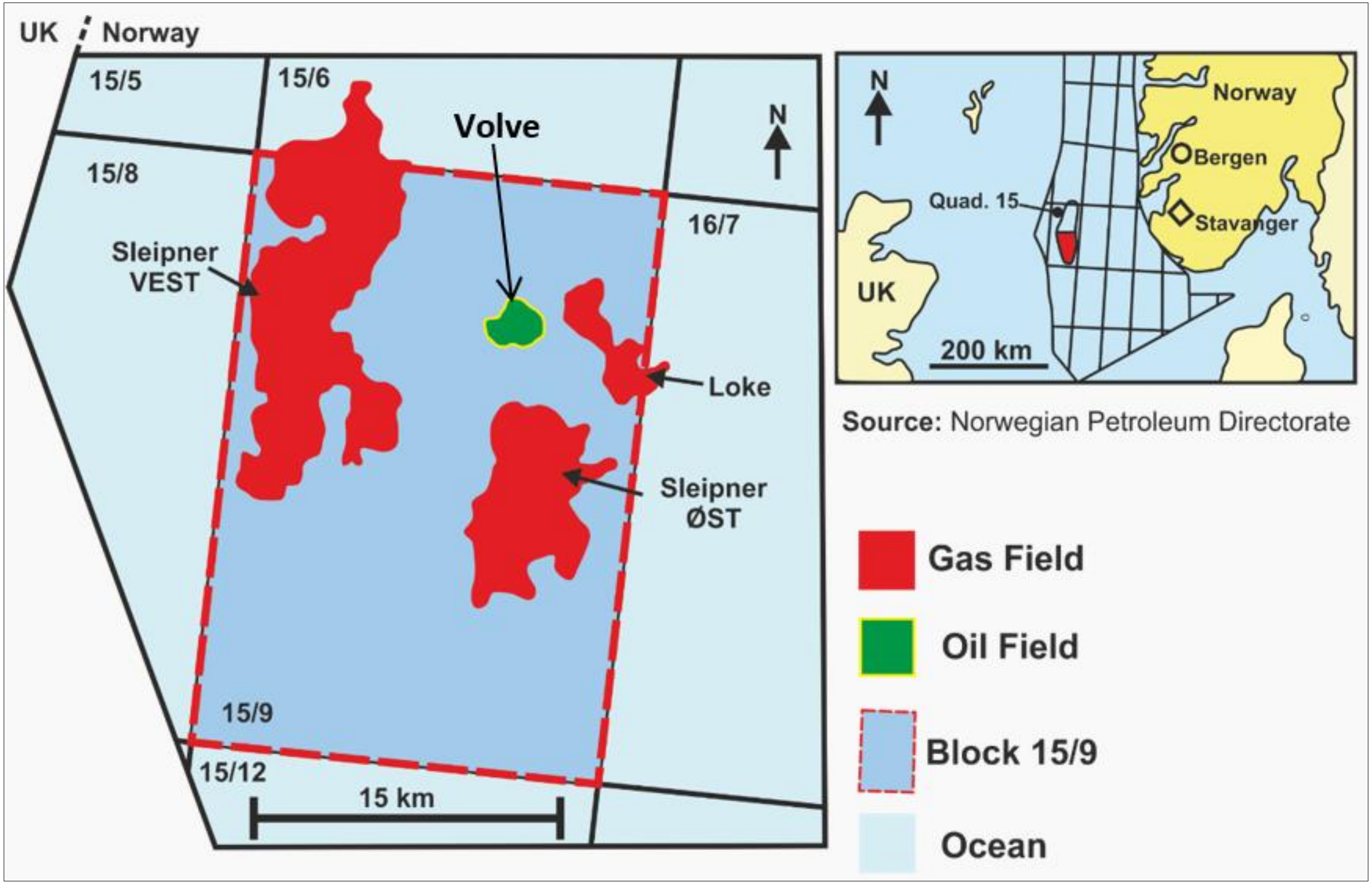

Fig 1. Location map of the Volve field~~,~~; showing gas and oil fields in quadrant 15/9, Norwegian North Sea (~~Adapted~~ from Ravasi et al., 2015).

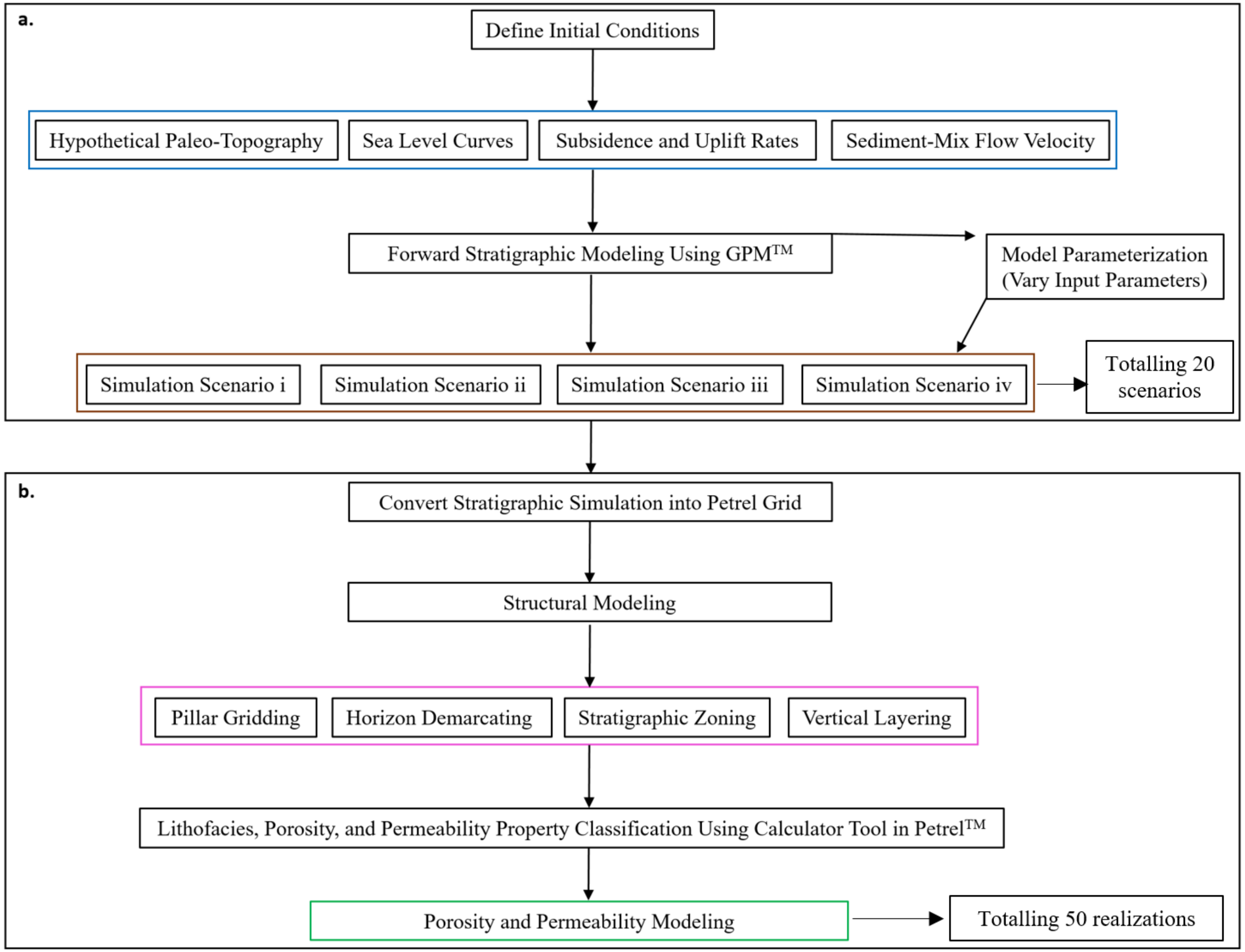
a.
Define Initial Conditions
Hypothetical Paleo-Topography
Sea Level Curves
Subsidence and Uplift Rates
Sediment-Mix Flow Velocity
Forward Stratigraphic Modeling Using GPM™
Model Parameterization (Vary Input Parameters)
Simulation Scenario i
Simulation Scenario ii
Simulation Scenario iii
Simulation Scenario iv
Totalling 20 scenarios
b.
Convert Stratigraphic Simulation into Petrel Grid
Structural Modeling
Pillar Gridding
Horizon Demarcating
Stratigraphic Zoning
Vertical Layering
Lithofacies, Porosity, and Permeability Property Classification Using Calculator Tool in Petrel™
Porosity and Permeability Modeling
Totalling 50 realizations

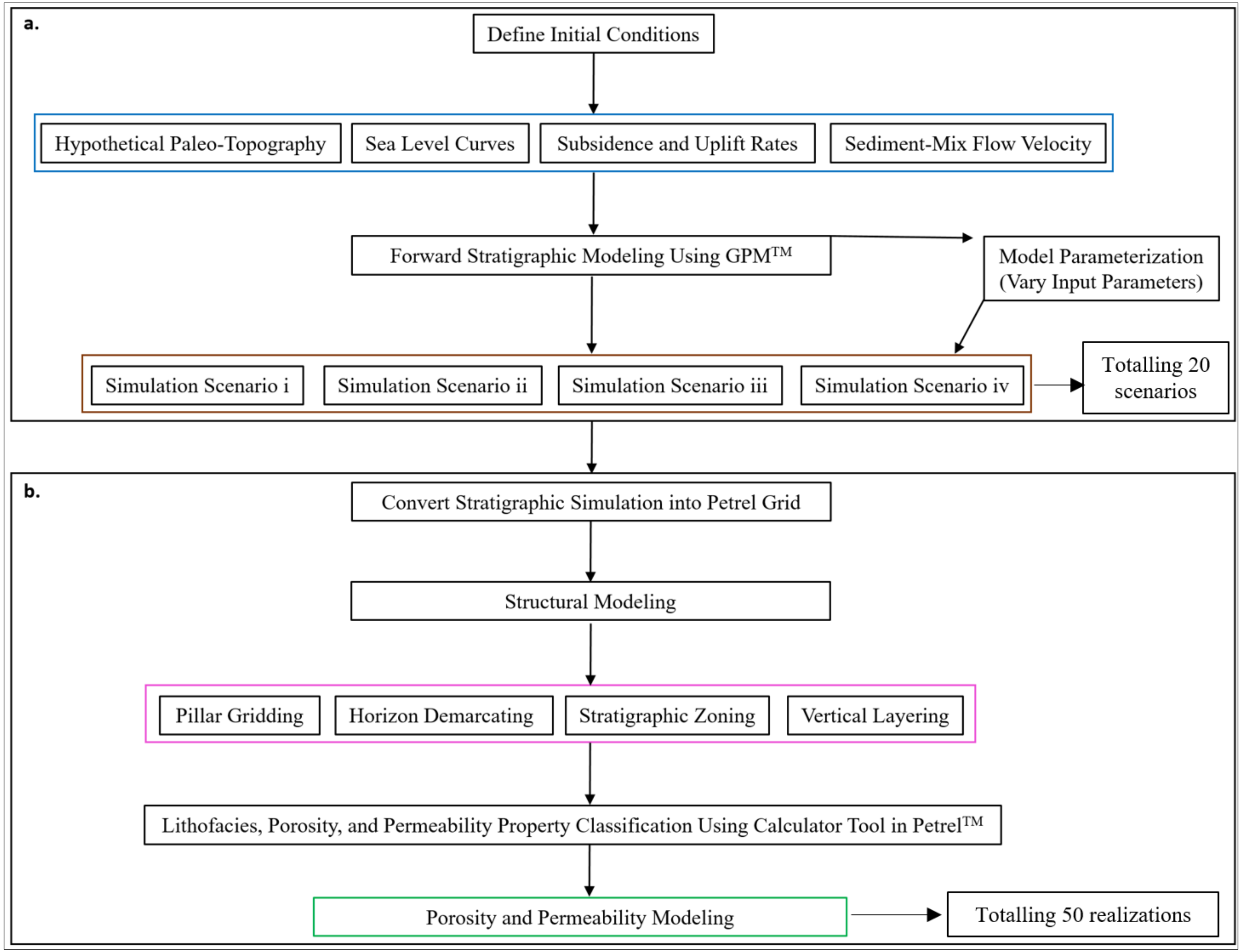
a.
Define Initial Conditions
Hypothetical Paleo-Topography
Sea Level Curves
Subsidence and Uplift Rates
Sediment-Mix Flow Velocity
Forward Stratigraphic Modeling Using GPM™
Model Parameterization (Vary Input Parameters)
Simulation Scenario i
Simulation Scenario ii
Simulation Scenario iii
Simulation Scenario iv
Totalling 20 scenarios
b.
Convert Stratigraphic Simulation into Petrel Grid
Structural Modeling
Pillar Gridding
Horizon Demarcating
Stratigraphic Zoning
Vertical Layering
Lithofacies, Porosity, and Permeability Property Classification Using Calculator Tool in Petrel™
Porosity and Permeability Modeling
Totalling 50 realizations

Fig 2. Schematic workflow of processes involved in this work. a. providing information of ~~initial~~boundary conditions (~~or~~ input parameters) ~~that were~~ used in the forward stratigraphic simulation in GPM^{TM}~~;~~; b. ~~demonstrating~~demonstrate how the forward stratigraphic ~~were~~model are converted into a grid that is usable in ~~the~~ Petrel^{TM} ~~environment~~ for ~~onward 3-D~~ porosity and permeability modeling.

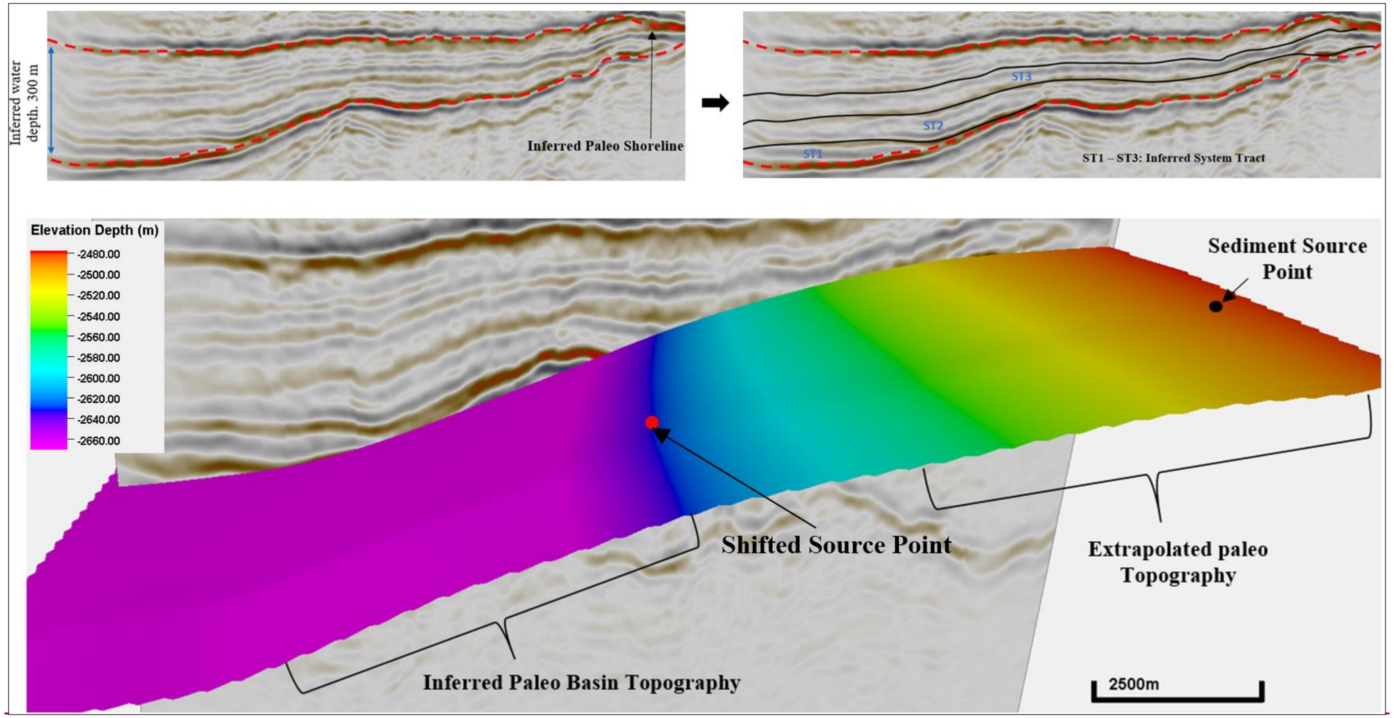

Inferred water depth. 300 m
Inferred Paleo Shoreline
ST3
ST2
ST1
ST1 – ST3: Inferred System Tract
Elevation Depth (m)
-2480.00
-2500.00
-2520.00
-2540.00
-2560.00
-2580.00
-2600.00
-2620.00
-2640.00
-2660.00
Sediment Source Point
Shifted Source Point
Extrapolated paleo Topography
Inferred Paleo Basin Topography
2500m

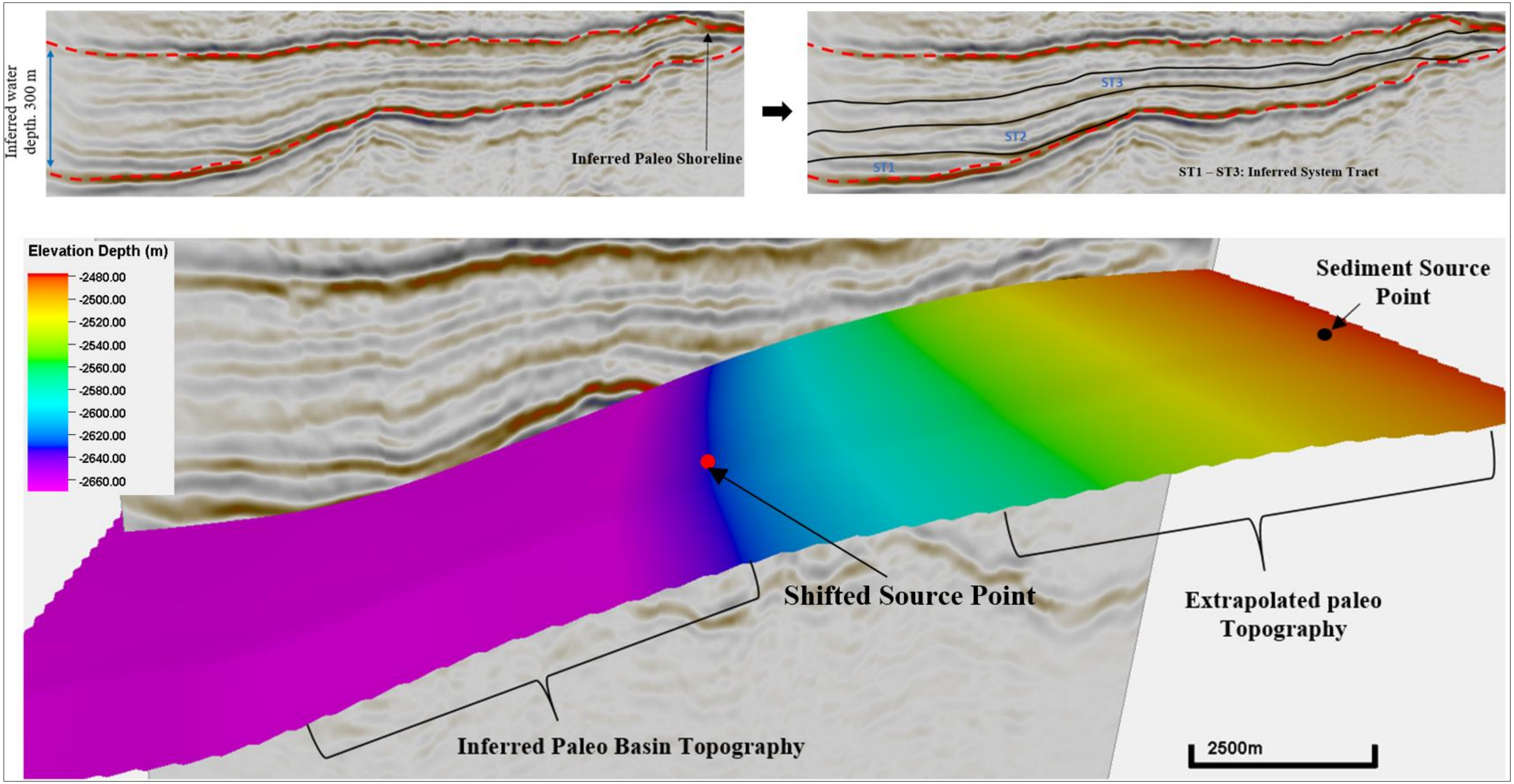

Fig 3. 3-D seismic section of the study area, from which the hypothetical topographic surface ~~was~~is derived for the simulation. The sedimentary entry point into the basin is located in the North Eastern section~~, ~~(based on ~~previous study in the model area (e.g. ~~Kieft et al. 2011).

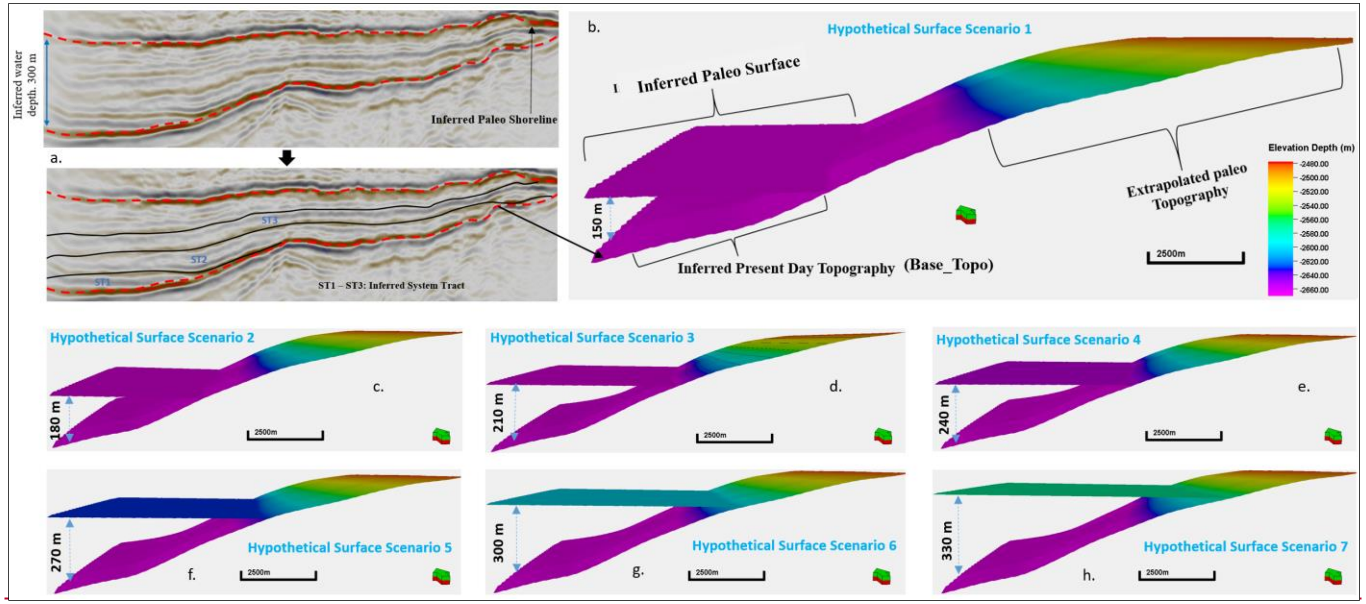

Inferred water depth. 300 m
Inferred Paleo Shoreline
a.
ST3
ST2
ST1
ST1 – ST3: Inferred System Tract
b.
Hypothetical Surface Scenario 1
Inferred Paleo Surface
Extrapolated paleo Topography
150 m
Inferred Present Day Topography (Base_Topo)
Elevation Depth (m)
-2480.00
-2500.00
-2520.00
-2540.00
-2560.00
-2580.00
-2600.00
-2620.00
-2640.00
-2660.00
2500m
Hypothetical Surface Scenario 2
c.
180 m
Hypothetical Surface Scenario 3
d.
210 m
Hypothetical Surface Scenario 4
e.
240 m
270 m
Hypothetical Surface Scenario 5
f.
300 m
Hypothetical Surface Scenario 6
g.
330 m
Hypothetical Surface Scenario 7
h.

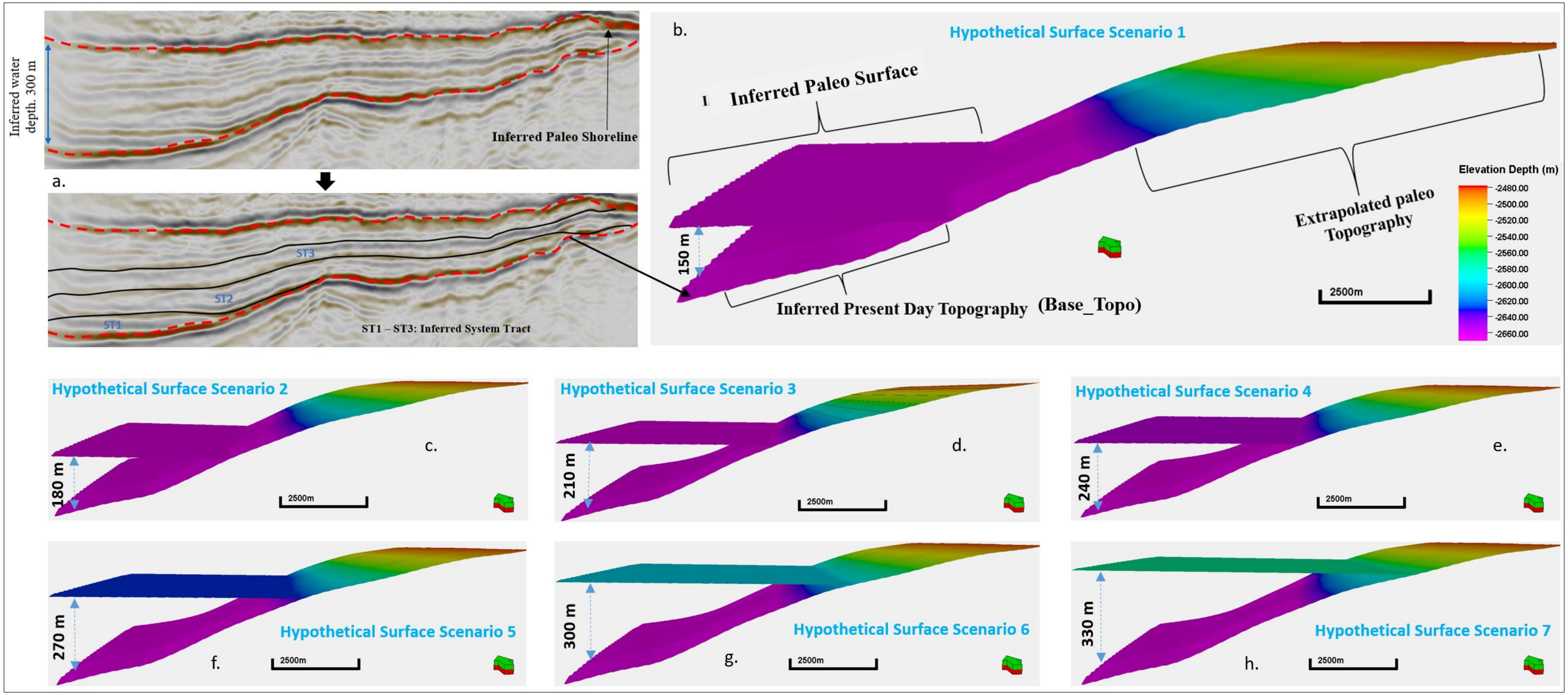

Fig 4. ~~Inferred paleo~~Paleo topographic surface from seismic~~, also~~. Also, illustrating different topographic surface scenarios ~~used in~~that are produced for the simulation.

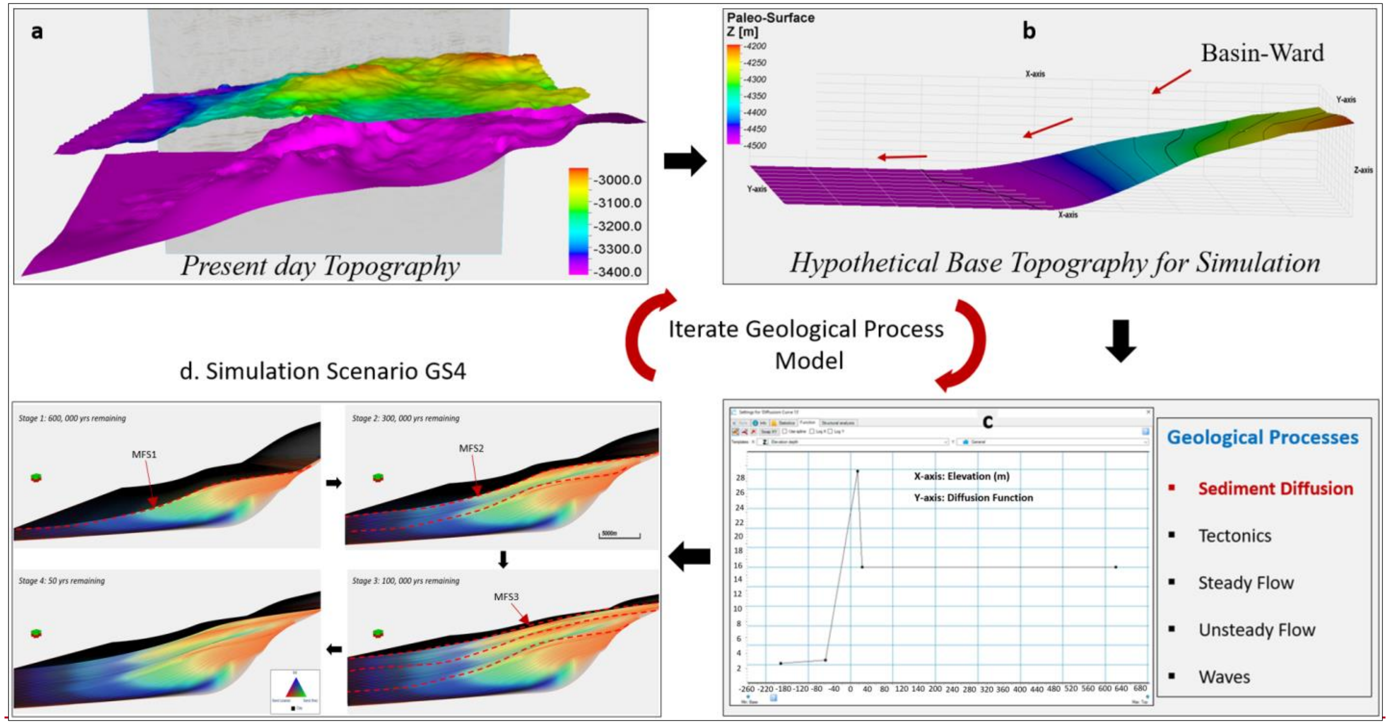
a
Present day Topography
-3000.0
-3100.0
-3200.0
-3300.0
-3400.0
Paleo-Surface
Z [m]
b
Basin-Ward
Hypothetical Base Topography for Simulation
Iterate Geological Process
Model
d. Simulation Scenario GS4
MFS1
MFS2
MFS3
c
X-axis: Elevation (m)
Y-axis: Diffusion Function
Geological Processes
Sediment Diffusion
Tectonics
Steady Flow
Unsteady Flow
Waves

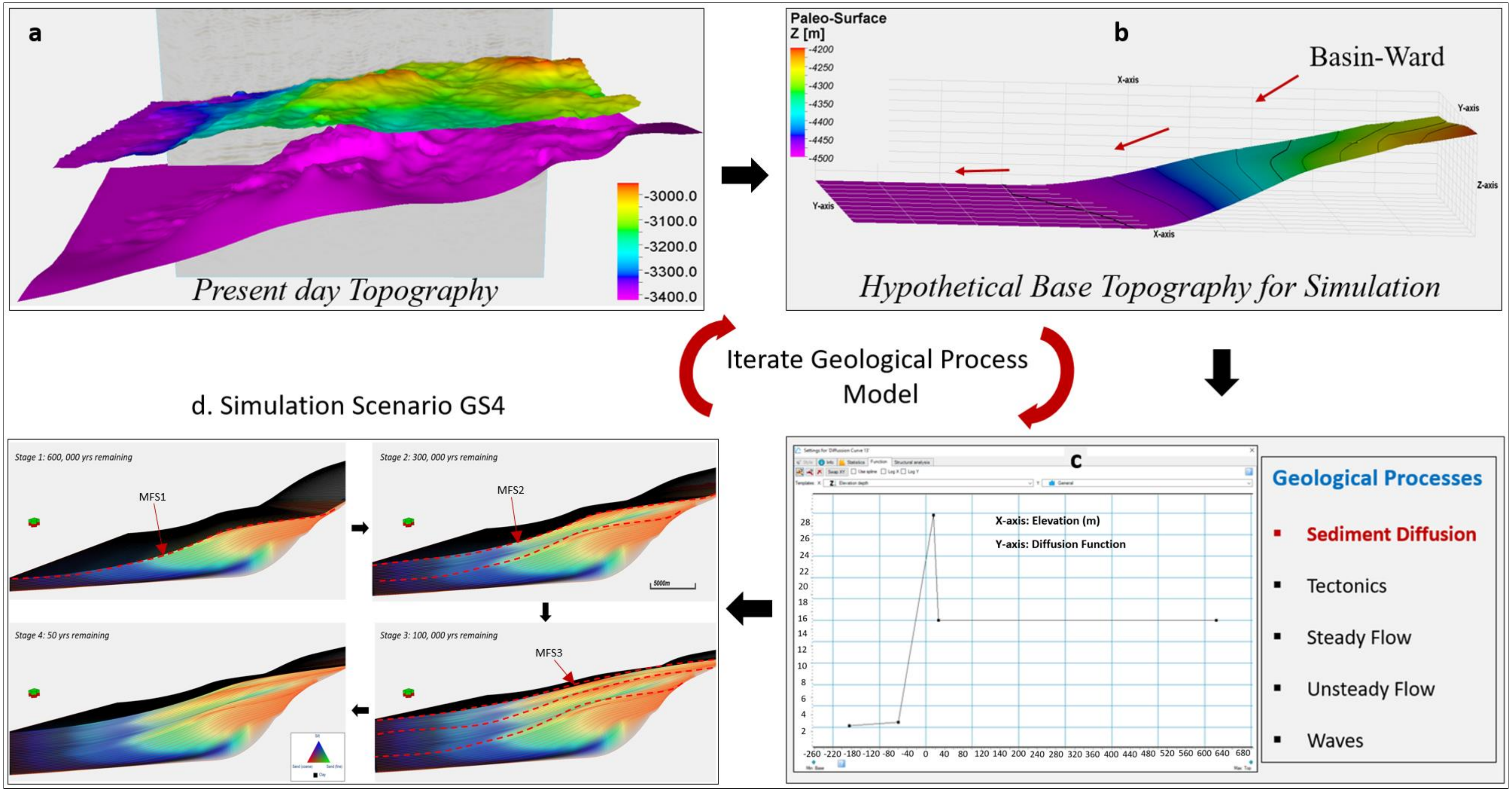

Fig 5. a. present-~~-~~day top and bottom topographic surfaces of the Hugin formation; b. hypothetical topographic surface ~~derived~~ from seismic data; c. geological processes involved in the forward stratigraphic simulation; d. forward stratigraphic models at different simulation time intervals.

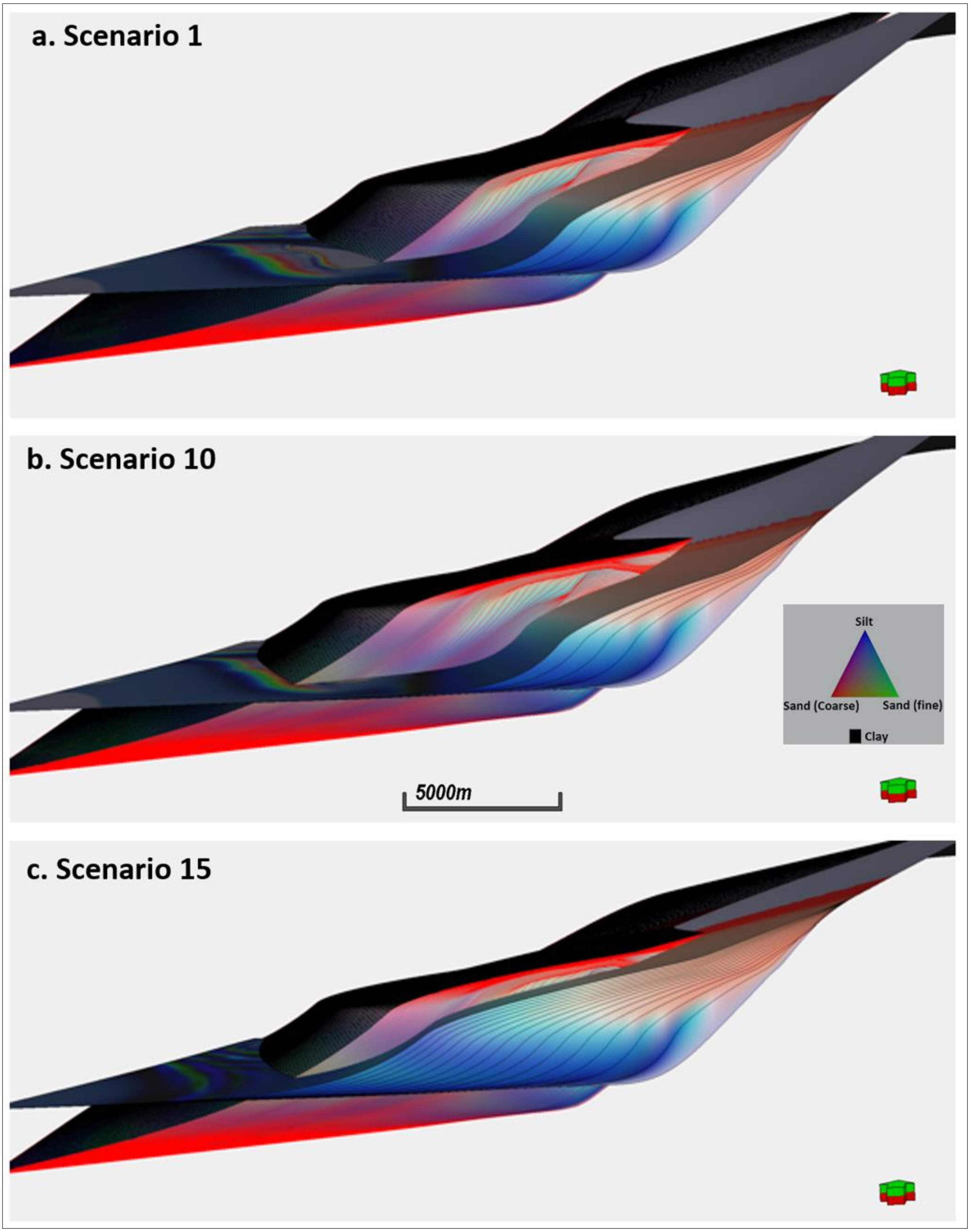

Fig 6. Stratigraphic simulation scenarios depicting sediment deposition in a shallow marine framework. **a.** scenario 1 involves equal proportions of sediment input, a relatively low subsidence rate and low water depth, **b.** scenario 10 uses high proportions of fine sand and silt (~~i.e.~~ 70%) in the sediment mix, abrupt changes in subsidence rate, and a relatively high water depth, c. scenario 15 involves very high proportions of fine sand and silt (~~i.e.~~ 80%), steady rate of subsidence and uplift in the sediment source area, and a relatively low water depth.

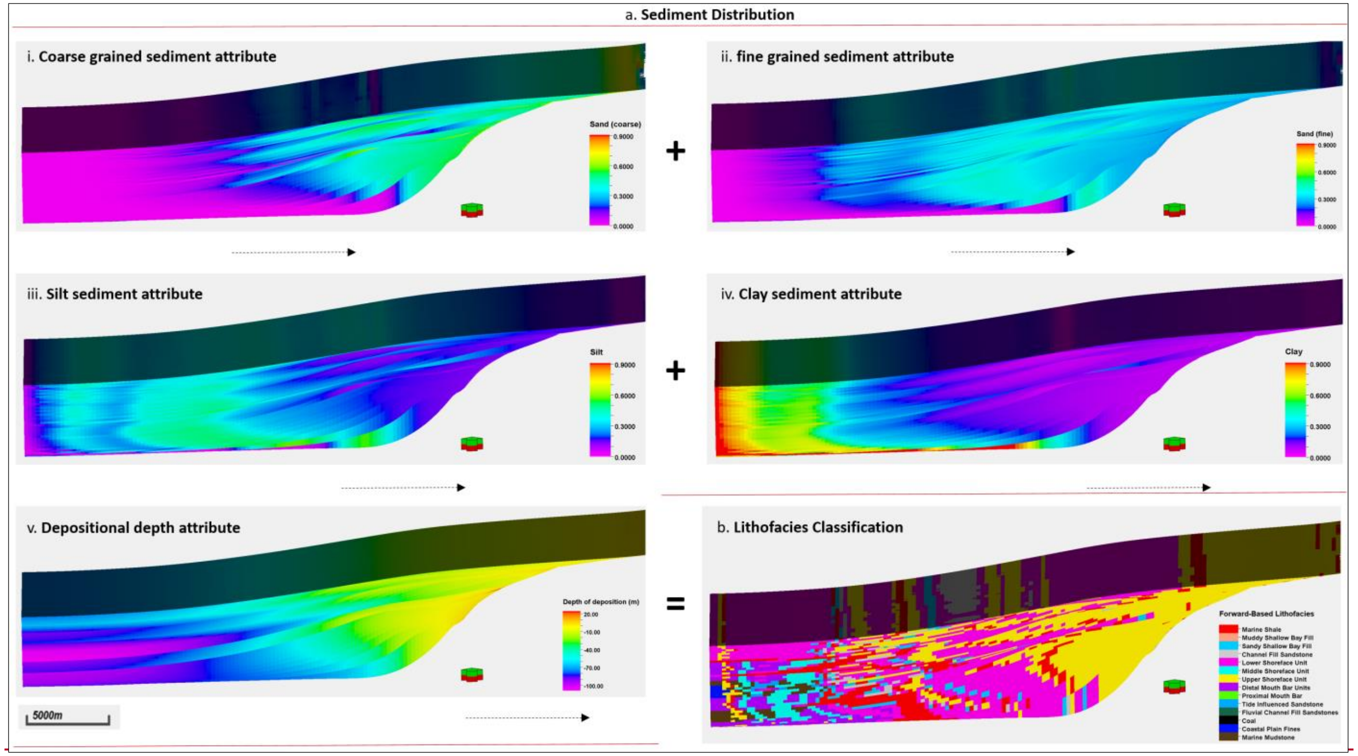

a. Sediment Distribution
i. Coarse grained sediment attribute
Sand (coarse)
0.9000
0.6000
0.3000
0.0000
+
ii. fine grained sediment attribute
Sand (fine)
0.9000
0.6000
0.3000
0.0000
iii. Silt sediment attribute
Silt
0.9000
0.6000
0.3000
0.0000
+
iv. Clay sediment attribute
Clay
0.9000
0.6000
0.3000
0.0000
v. Depositional depth attribute
Depth of deposition (m)
20.00
-10.00
-40.00
-70.00
-100.00
=
b. Lithofacies Classification
Forward-Based Lithofacies
Marine Shale
Muddy Shallow Bay Fill
Sandy Shallow Bay Fill
Channel Fill Sandstone
Lower Shoreface Unit
Middle Shoreface Unit
Upper Shoreface Unit
Distal Mouth Bar Units
Proximal Mouth Bar
Tide Influenced Sandstone
Fluvial Channel Fill Sandstones
Coal
Coastal Plain Fines
Marine Mudstone
5000m

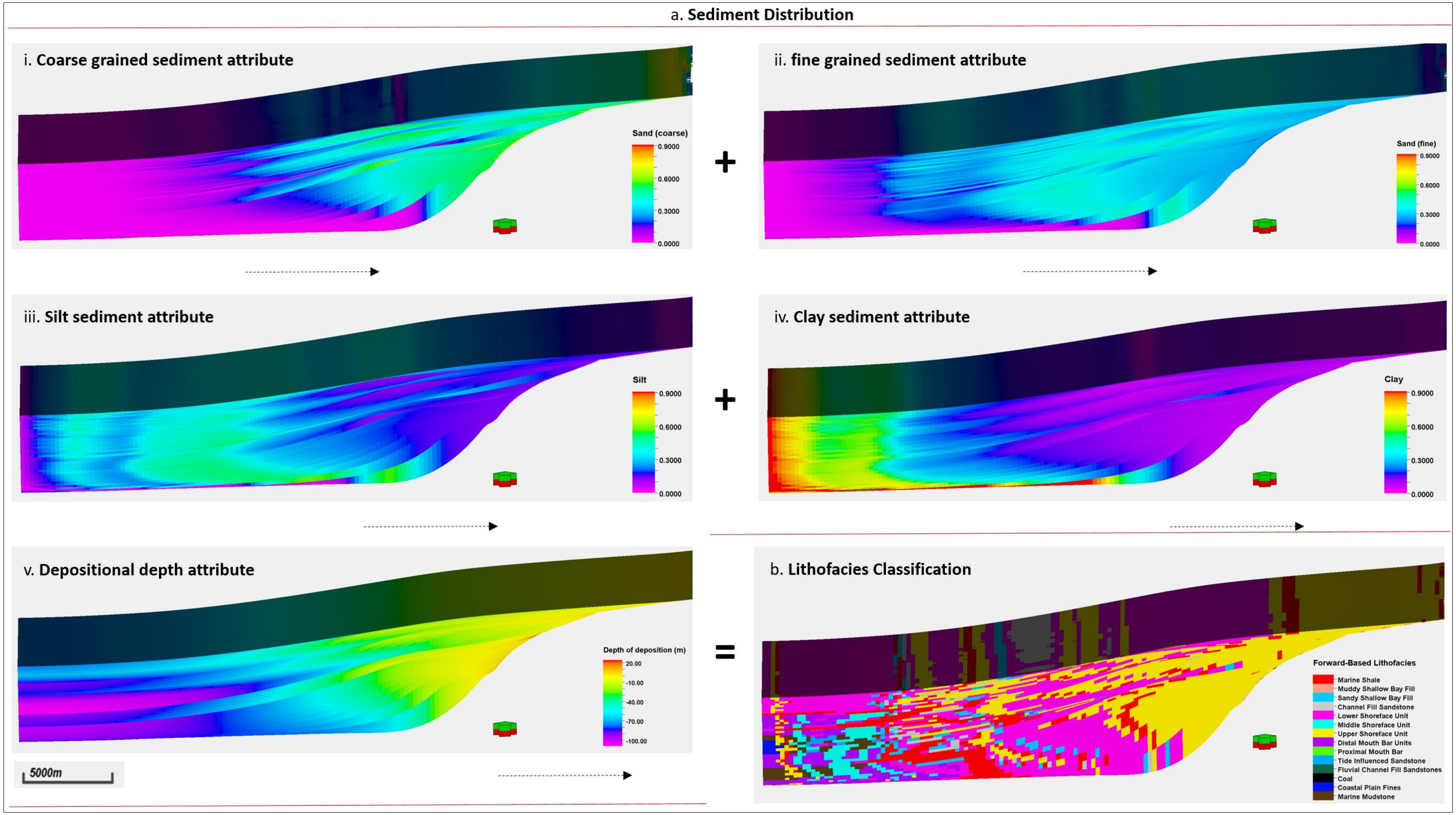

Fig 7 a. Sediment distribution patterns in the geological process modeling software. b. lithofacies classification using the property calculator tool in Petrel™.

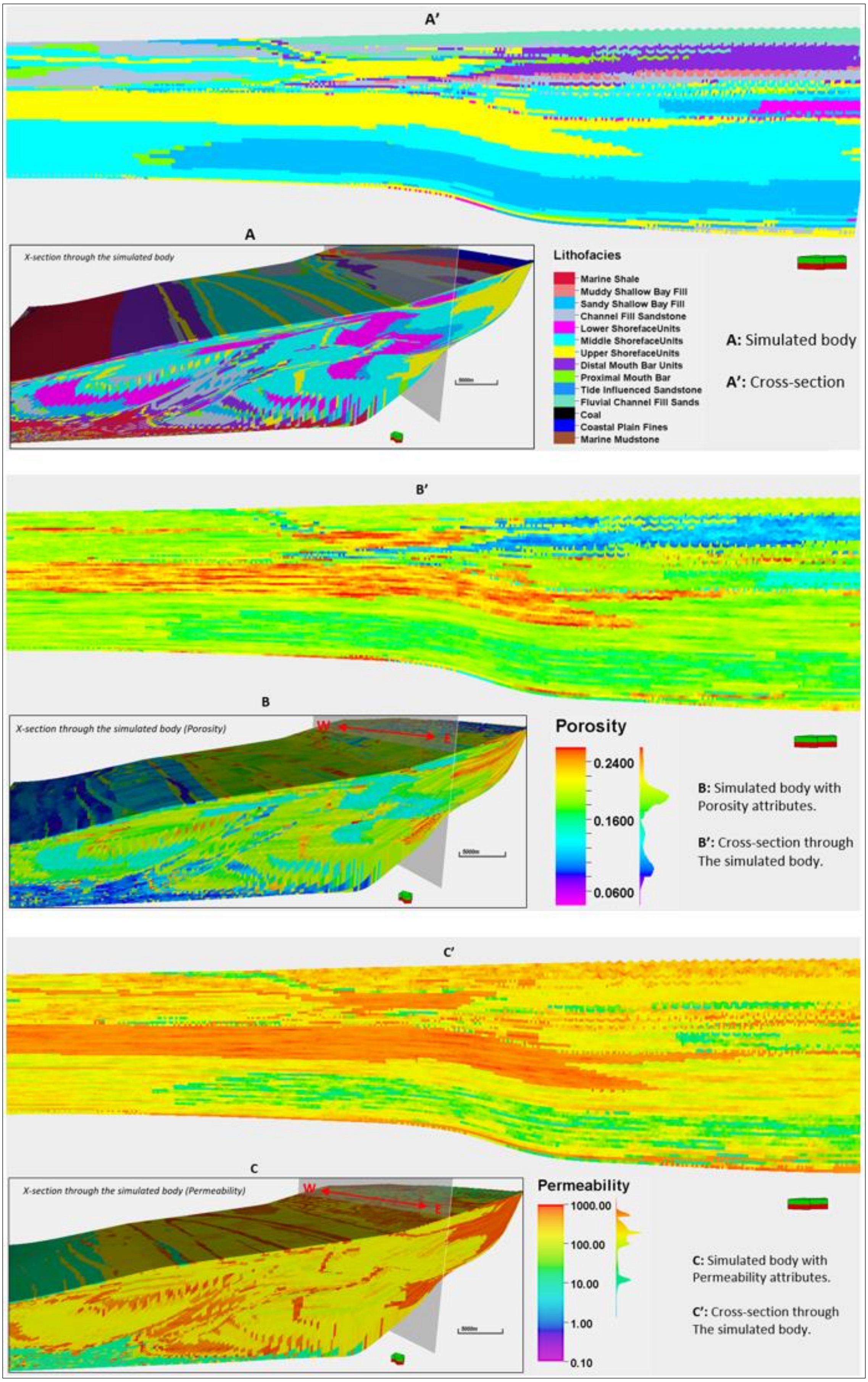
A'
A
X-section through the simulated body
Lithofacies
Marine Shale
Muddy Shallow Bay Fill
Sandy Shallow Bay Fill
Channel Fill Sandstone
Lower ShorefaceUnits
Middle ShorefaceUnits
Upper ShorefaceUnits
Distal Mouth Bar Units
Proximal Mouth Bar
Tide Influenced Sandstone
Fluvial Channel Fill Sands
Coal
Coastal Plain Fines
Marine Mudstone
A: Simulated body
A': Cross-section
B'
B
X-section through the simulated body (Porosity)
W
E
Porosity
0.2400
0.1600
0.0600
B: Simulated body with Porosity attributes.
B': Cross-section through The simulated body.
C'
C
X-section through the simulated body (Permeability)
Permeability
1000.00
100.00
10.00
1.00
0.10
C: Simulated body with Permeability attributes.
C': Cross-section through The simulated body.

Fig 8. ~~Property~~Lithofacies, porosity and permeability characterization in the stratigraphic ~~using~~model through the property calculator tool in ~~Petrel~~Petrel™. Also~~ showing~~, is a cross-sectional view ~~through~~of the ~~model~~3-D models.

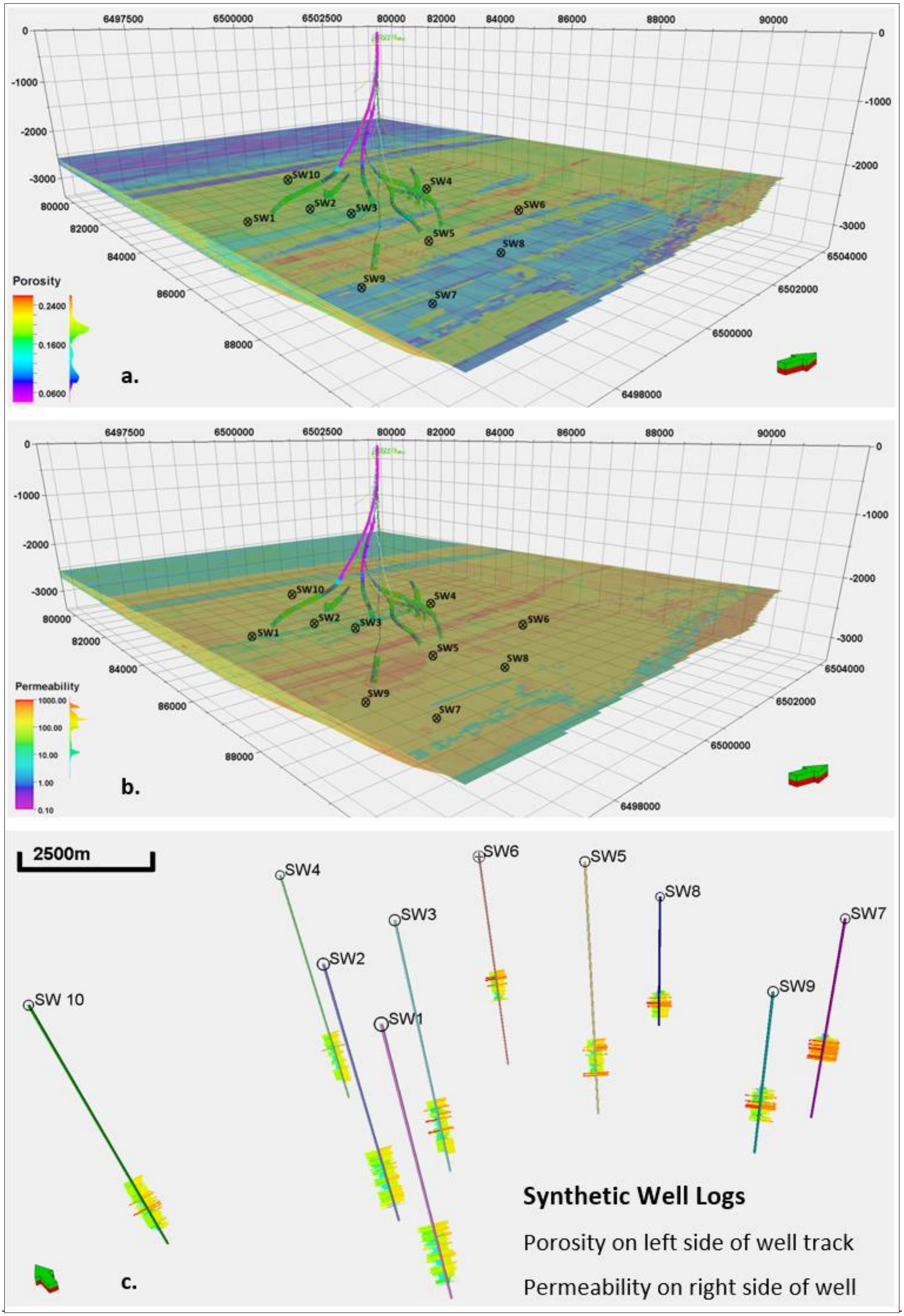

Porosity
0.2400
0.1600
0.0600
a.
SW10
SW1
SW2
SW3
SW4
SW5
SW6
SW7
SW8
SW9
Permeability
1000.00
100.00
10.00
1.00
0.10
b.
2500m
SW 10
c.
Synthetic Well Logs
Porosity on left side of well track
Permeability on right side of well

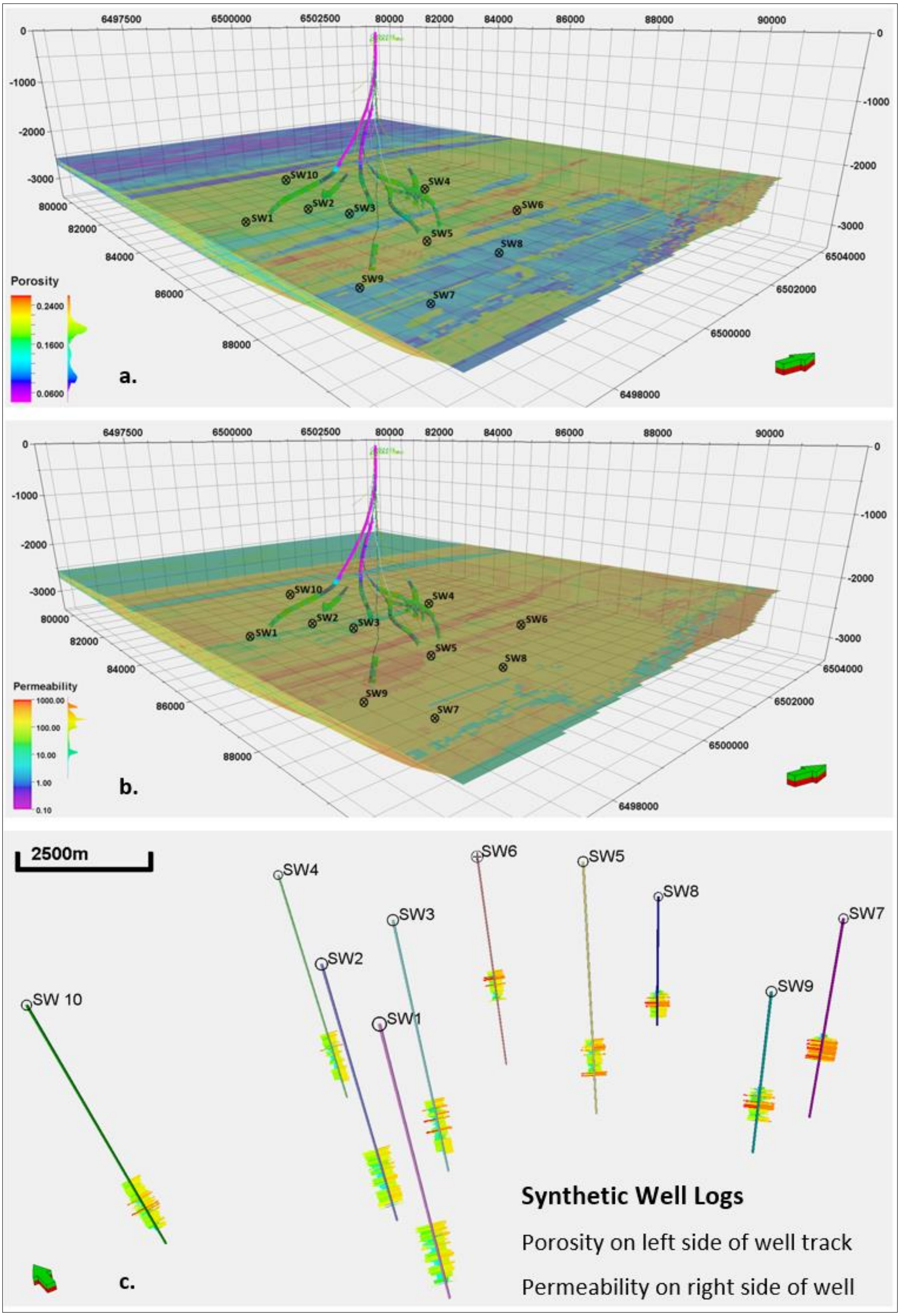

Fig 9. Synthetic wells ~~derived~~ from a forward stratigraphic-driven porosity and permeability ~~models.~~

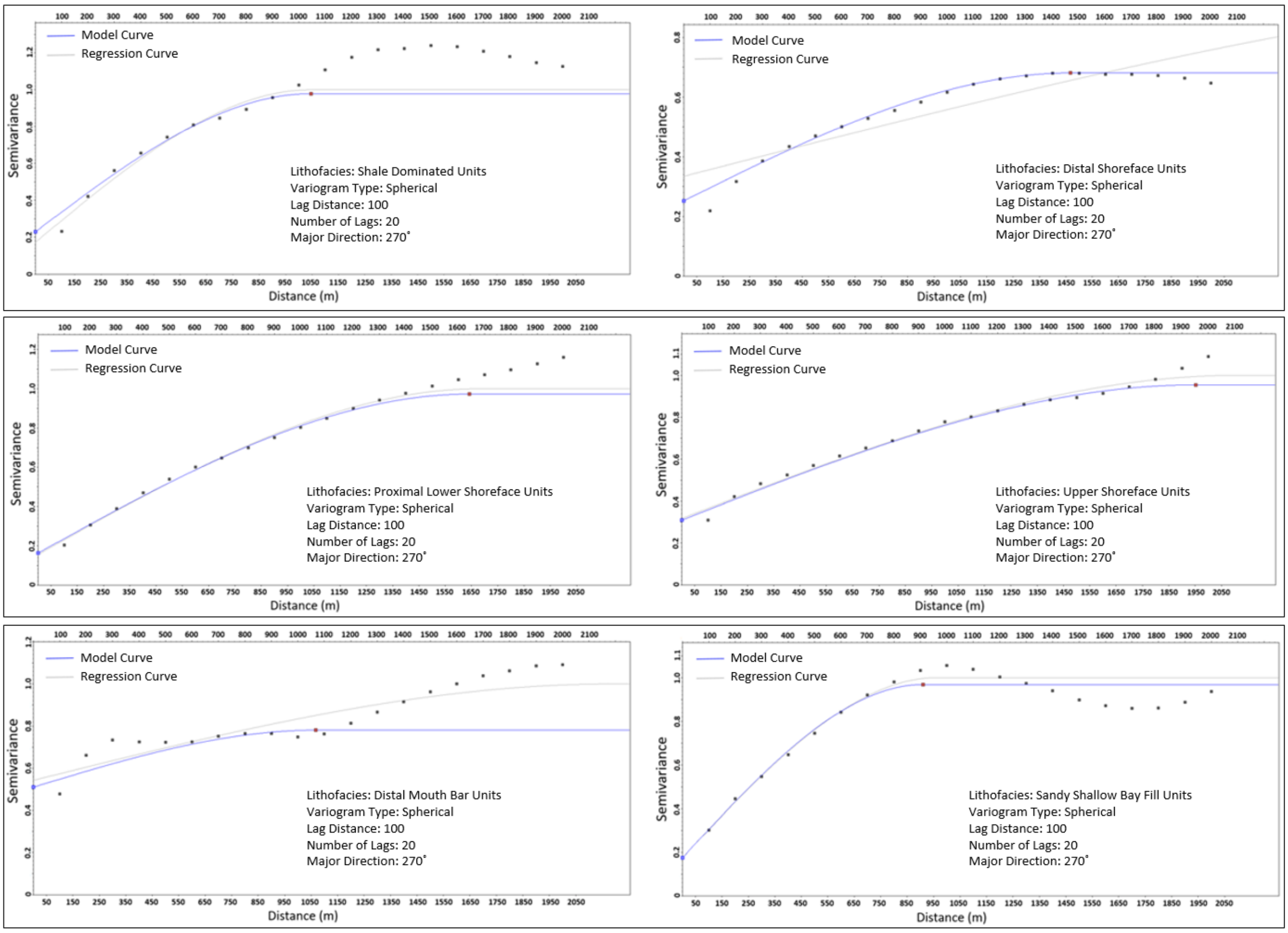

model. The average separation distance between the synthetic wells shown in Figure 9c is about 0.9 km apart (maximum and minimum separation distance of 1.3 km and 0.65 km, respectively).

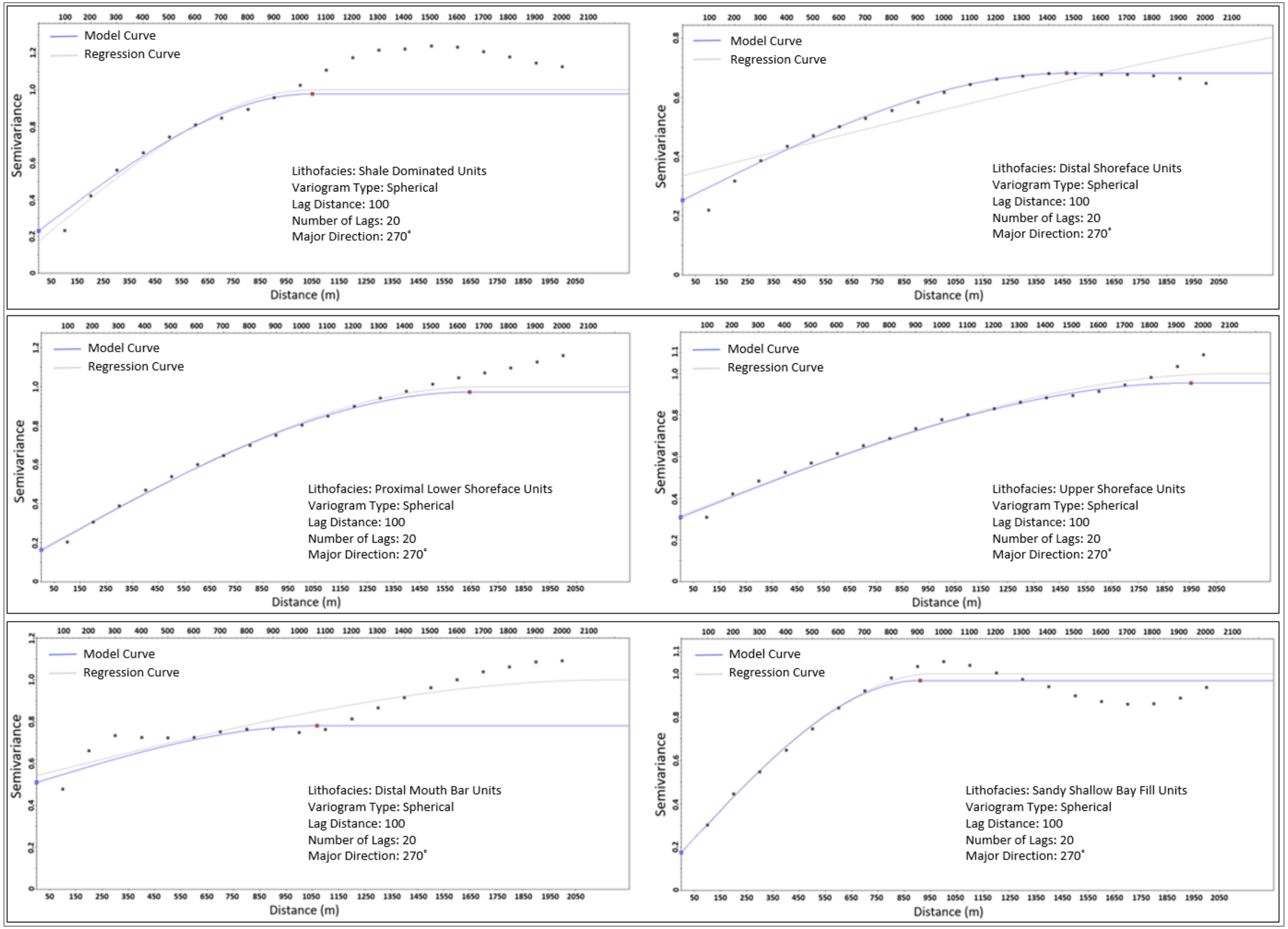
Model Curve
Regression Curve
Semivariance
Distance (m)
Lithofacies: Shale Dominated Units
Variogram Type: Spherical
Lag Distance: 100
Number of Lags: 20
Major Direction: 270˚
Lithofacies: Distal Shoreface Units
Variogram Type: Spherical
Lag Distance: 100
Number of Lags: 20
Major Direction: 270˚
Lithofacies: Proximal Lower Shoreface Units
Variogram Type: Spherical
Lag Distance: 100
Number of Lags: 20
Major Direction: 270˚
Lithofacies: Upper Shoreface Units
Variogram Type: Spherical
Lag Distance: 100
Number of Lags: 20
Major Direction: 270˚
Lithofacies: Distal Mouth Bar Units
Variogram Type: Spherical
Lag Distance: 100
Number of Lags: 20
Major Direction: 270˚
Lithofacies: Sandy Shallow Bay Fill Units
Variogram Type: Spherical
Lag Distance: 100
Number of Lags: 20
Major Direction: 270˚

Fig 10. Variogram model of dominant lithofacies units ~~extracted~~ from the ~~FSM~~forward stratigraphic model. The points indicate the number of lags in the variogram. The distance between these lags is about 100 m. This figure shows the lags between sample pairs for calculating the variogram in the major direction (NE-SW) of the stratigraphic model.

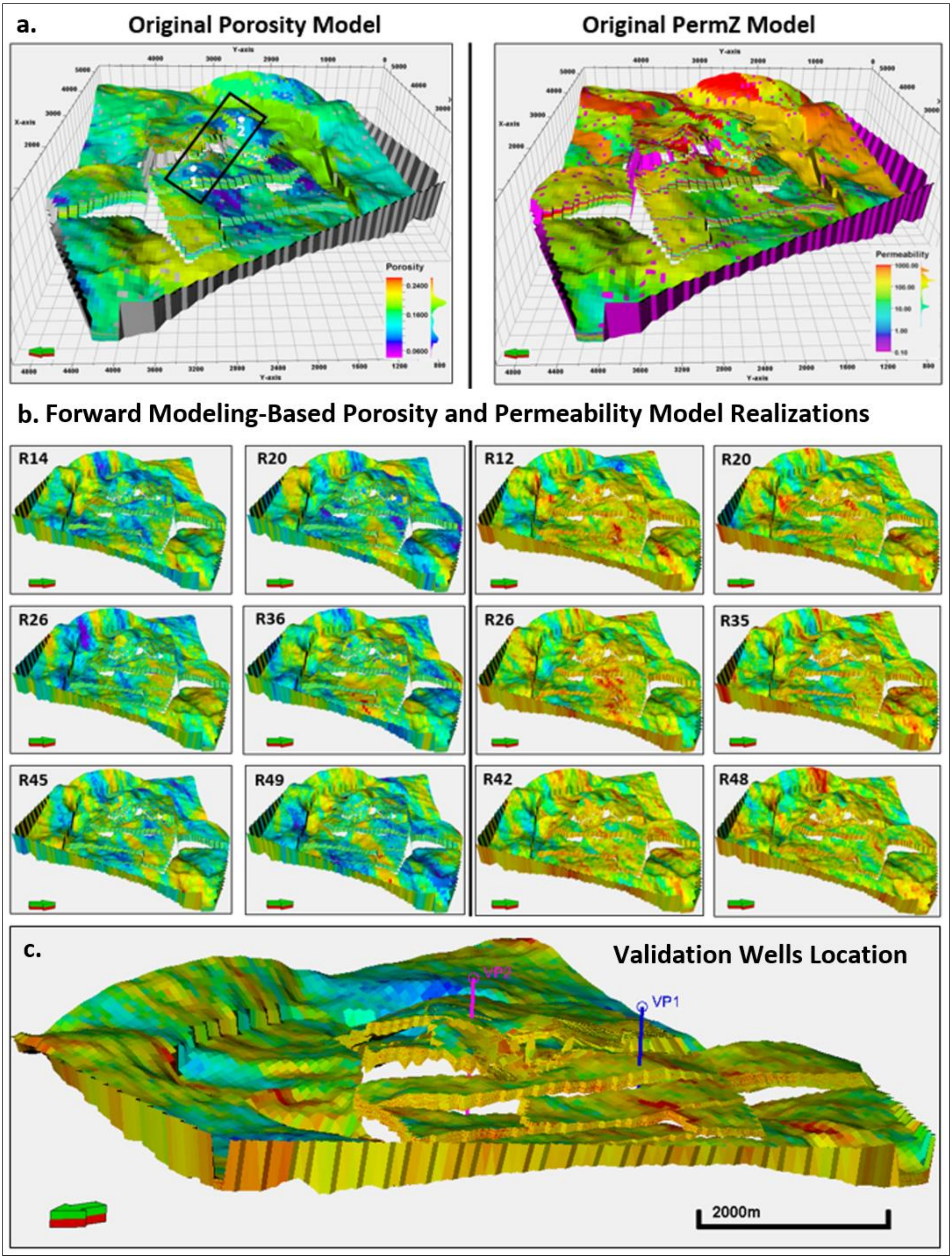

a.
Original Porosity Model
Original PermZ Model
Porosity
Permeability
b. Forward Modeling-Based Porosity and Permeability Model Realizations
R14
R20
R12
R20
R26
R36
R26
R35
R45
R49
R42
R48
c.
Validation Wells Location
VP2
VP1
2000m

Fig 11. ~~Comparing original~~Original Volve field model ~~to~~vs the forward modeling-based models. Realizations 16, 20, 26, 36, 45, and 49 on the left half are porosity models, ~~whilst~~whiles realizations 12, 20, 26, 35, 42, and 48 on the right half ~~show~~are permeability models.

a. Validation Well 1

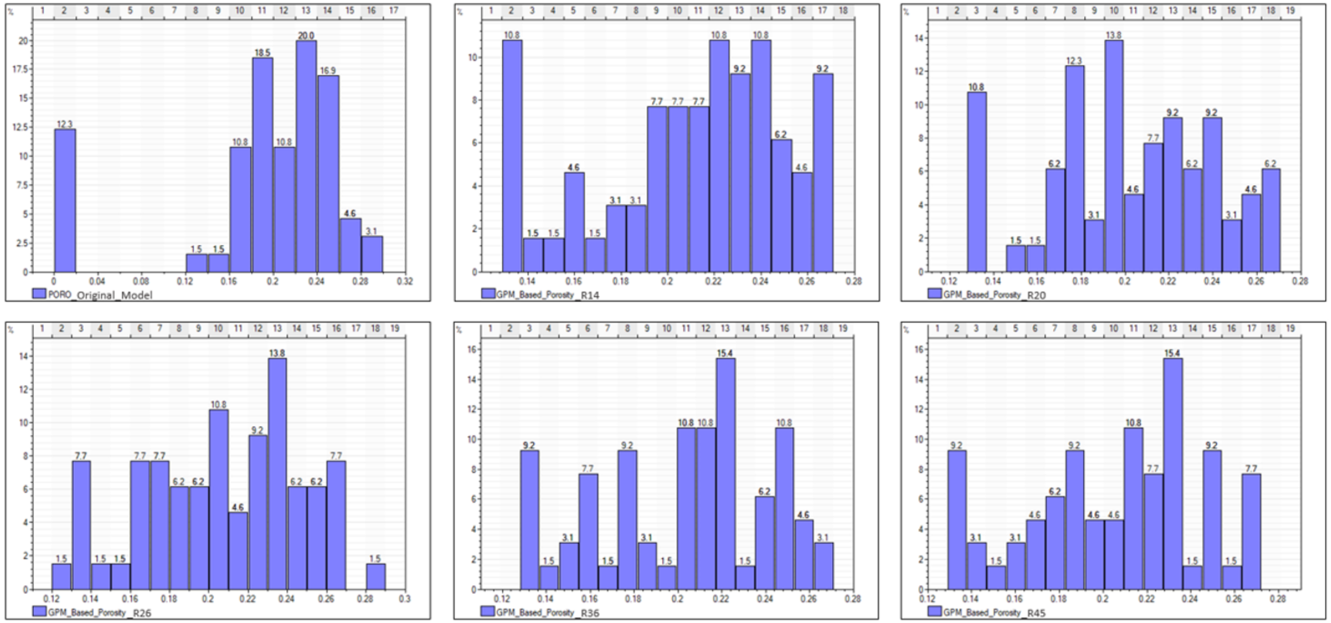

b. Validation Well 2

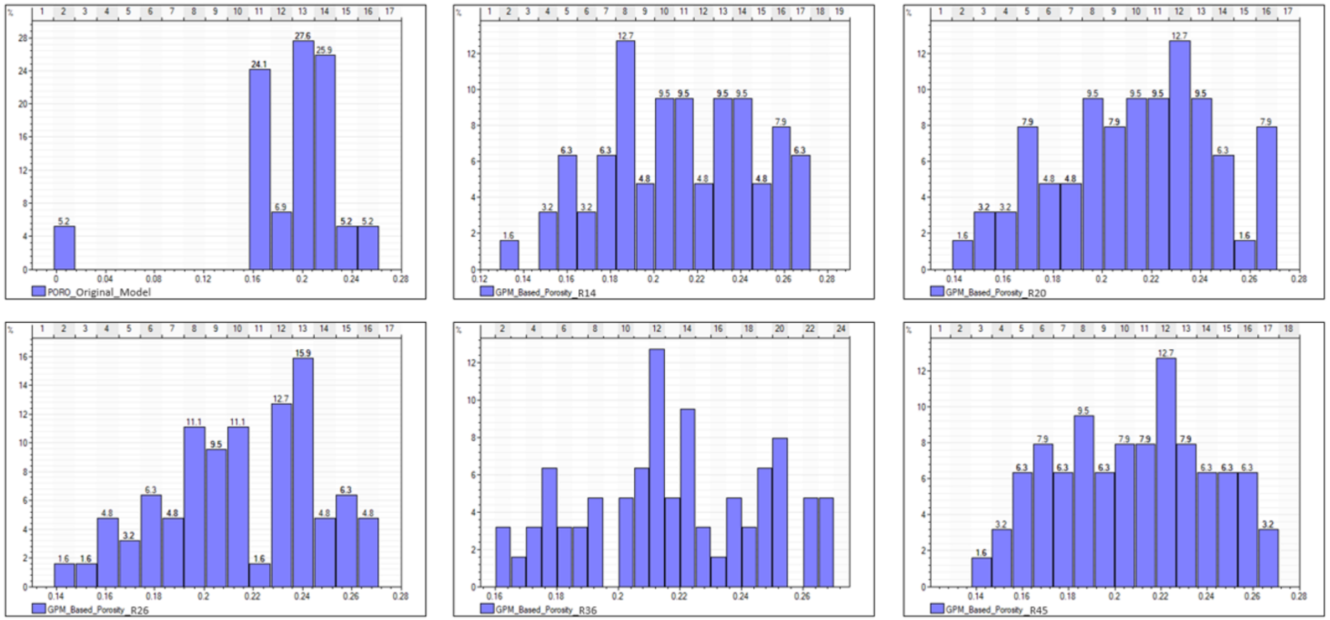

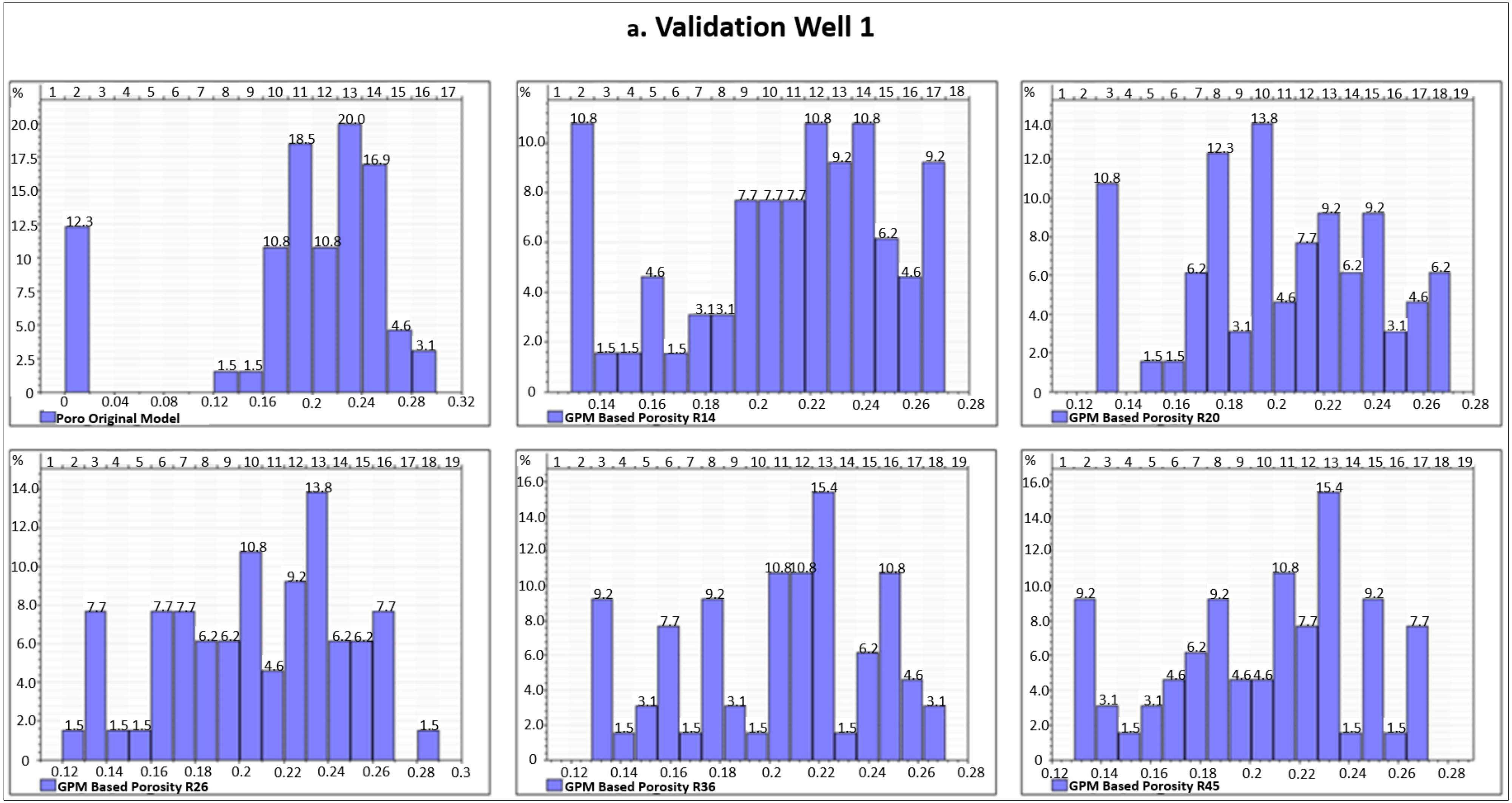

Figure ~~12. Illustrating how; a.~~ 12a. Comparing porosity in validation ~~well~~Well 1 in five stratigraphic-based realizations, and ~~b.~~ the original model at similar vertical intervals.

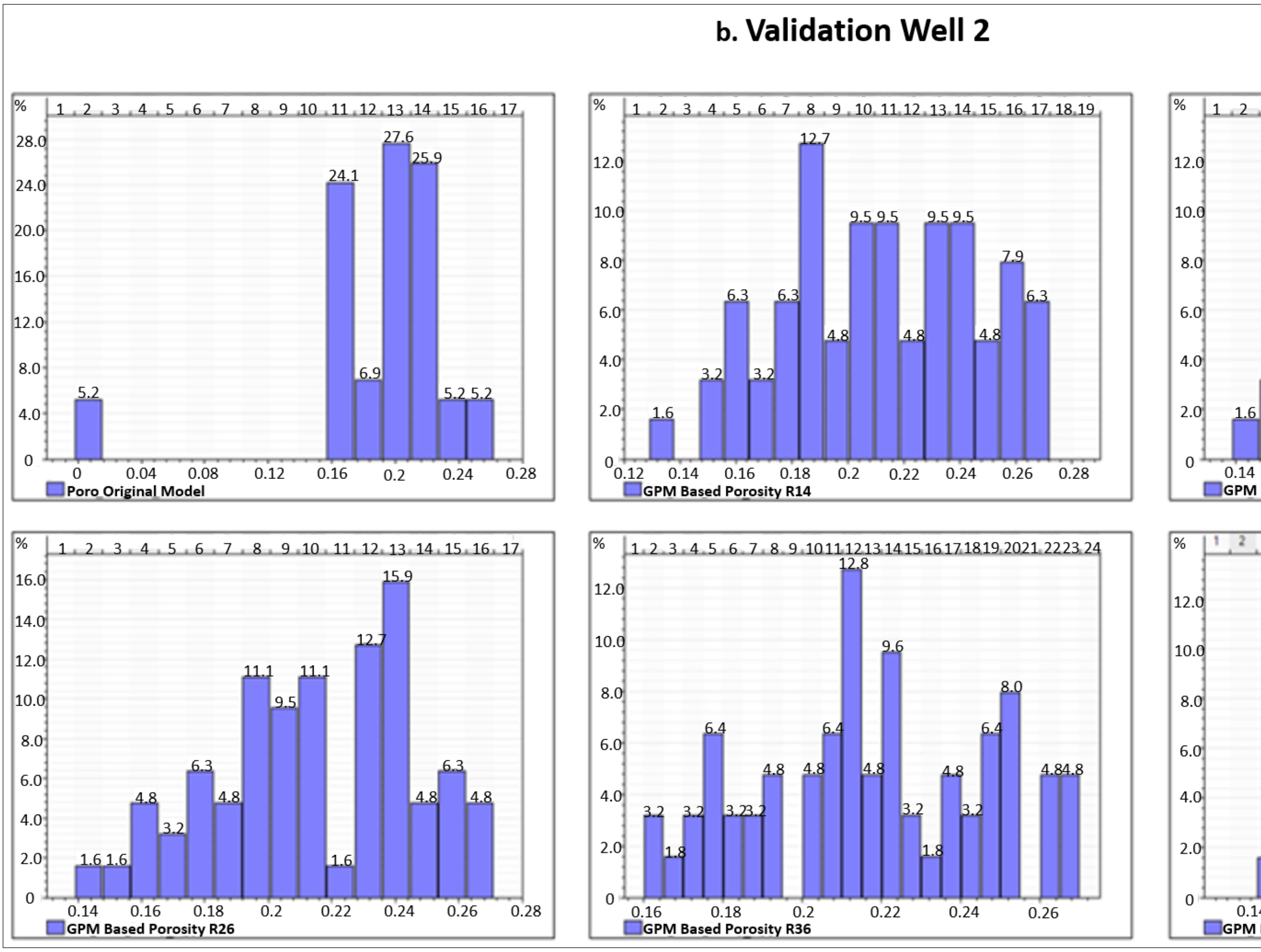

Figure 12b. Comparing porosity in validation ~~well~~Well 2 ~~samples~~ in ~~the synthetic forward~~ five stratigraphic-based ~~model compares to pseudo wells from~~realizations, and the original ~~Volve field petrophysical~~ model~~.~~

at similar vertical intervals.

Code	Facies	Description	Thickness (t); extent (l)	Wireline-log Attribute	Interpretation
A	A1	Parallel-laminated mudstone with occasional siltstone inputs. Monospecific pattern of disorder bivalves parallel to bedding.	t= 30-425 cm l= 6 to 29 km	GR= 41-308 API DT= 225-355 µsm^{-1} NPHI= 0.17-0.45 v/v RHOB= 2280-2820 gcm^{-3}	Restricted marine shale
	A2	Interbedded claystone and very fine-grained sandstone; non-parallel and wavy lamination. Scarcely bivalve shells oriented parallel to bedding.	t= 10-725 cm l = 8 km to 13 km	GR= 71-65 API DT= 189-268 µsm^{-1} NPHI=? RHOB= 2280-2820 gcm^{-3}	Muddy Shallow bay-fill
	A3	Fine to medium grained sandstone; moderately to well sorted grains. Wavy bedding, cross bedding, rare wave ripples	t= 60-370 cm l <8 km	GR= 18-46 API DT= 199-314 µsm^{-1} NPHI= 0.07-0.52 v/v RHOB= 1690-2745 gcm^{-3}	Sandy shallow bay-fill
	A4	Coarse to fine-grained sandstones with alternating upward fining to coarsening trend. Moderately sorted grains. Sparse sedimentary structures.	t= 250-500 cm l = 1.8 km to 4.2 km	GR= 7-35 API DT= 175-230 µsm^{-1} NPHI= 0.038-0.146 v/v RHOB= 2280-2820 gcm^{-3}	Marine channel-fill sandstones
B	B1	Upward-coarsening siltstone to fine-grained moderate sorted sandstones, with shell debris, and quartz granules.	t= 30-480 cm l = <2 km	GR= 18-80 API DT= 168-291 µsm^{-1} NPHI= 0.038-0.191 v/v RHOB= 2322-2723 gcm^{-3}	Distal lower shoreface
	B2	Very fine-fine grained, moderate to well sorted sandstone. Fine grained carbonaceous laminae, typically low angle cross beds.	t= 130-440 cm l = 1.7 km – 8 km	GR= 20-56 API DT= 179-277 µsm^{-1} NPHI= 0.048-0.168 v/v RHOB= 2314-2696 gcm^{-3}	Proximal lower shoreface
	B3	Coarsening upward, cross laminated, fine to medium grained, well sorted sandstone; consist carbonaceous fragments	t= 425-800 cm l = 1.7 km – 8 km	GR= 15-25 API DT= 250-275 µsm^{-1} NPHI= 0.09-0.113 v/v RHOB= 2271-2342 gcm^{-3}	Upper Shoreface
	C1	Highly bioturbated siltstone to very fine sandstones, which has beds of rounded granules	t= 175-1010 cm l = 7.2 km – 19.6 km	GR= 20-80 API DT= 230-260 µsm^{-1} NPHI= 0.08-0.169 v/v RHOB= 2327-2521 gcm^{-3}	Distal mouth bar

Table 1 Lithofacies-associations in the Hugin formation, Volve Field (after Kieft et al. 2011).

Code	Facies	Description	Thickness (t); Extent (l)	Wireline-log Attribute	Interpretation
A	A1	Parallel-laminated mudstone with occasional siltstone inputs. Monospecific pattern of disorder bivalves parallel to bedding.	t = 30 - 425 cm l = 6 - 29 km	GR = 41 - 308 API DT = 225 - 355 µsm^{-1} NPHI = 0.17 - 0.45 v/v RHOB = 2280 - 2820 gcm^{-1}	Restricted marine shale
	A2	Inter-bedded claystone and very fine-grained sandstone; non-parallel and wavy lamination. Scarecely bivalve shells oriented parallel to bedding.	t = 10 - 725 cm l = 8 - 13 km	GR = 17 - 65 API DT = 189 - 268 µsm^{-1} NPHI =? RHOB = 2280 - 2820 gcm-1	Muddy hallow bay fill
	A3	Fine to medium grained sandstone; moderately to well sorted grain. Wavy bedding, cross bedding, rare wave ripples.	t = 60 - 370 cm l = 1 - 8 km	GR = 18 - 46 API DT = 199 - 268 µsm^{-1} NPHI = 0.07 - 0.52 v/v RHOB = 1690 - 2745 gcm-1	Sandy shallow bay fill
	A4	Parallel-laminated mudstone with occasional siltstone inputs. Monospecific pattern of disorder bivalves parallel to bedding.	t = 30 - 425 cm l = 6 - 29 km	GR = 7 - 35 API DT = 175 - 230 µsm^{-1} NPHI = 0.04 - 0.15 v/v RHOB = 2280 - 2820 gcm-1	Marine channel fill sandstone
B	B1	Upward coarsening siltstone to fine-grained; moderatley sorted sandstone. Shell debris and quartz granules.	t = 30 - 480 cm l = 1 - 2 km	GR = 18 - 80 API DT = 168 - 291 µsm^{-1} NPHI = 0.04 - 0.191 v/v RHOB = 2322 - 2723 gcm-1	Distal lower shoreface
	B2	Very fine-fine grained sandstone. Moderate to well sorted; fine grained carbonaceous laminae, typically low angle cross beds.	t = 130 - 440 cm l = 1.7 - 12 km	GR = 20 - 56 API DT = 179 - 277 µsm^{-1} NPHI = 0.05 - 0.168 v/v RHOB = 2314 - 2696 gcm-1	Proximal lower shoreface
	B3	Coaesening upward, cross laminated, fine to medium grainned sandstone; consist of carbonaceous fragments.	t = 425 - 800 cm l = 1.7 - 8 km	GR = 15 - 25 API DT = 250 - 275 µsm^{-1} NPHI = 0.09 - 0.113 v/v RHOB = 2271 - 2342 gcm-1	Upper shoreface
C	C1	Highly bioturbated siltstone to very fine sandstone, with beds of rounded granules.	t = 175 - 1010 cm l = 7.2 - 19.6 km	GR = 20 - 80 API DT = 230 - 260 µsm^{-1} NPHI = 0.08 - 0.169 v/v RHOB = 2327 - 2521 gcm-1	Distal mouth bar
	C2	Very fine to fine grained sandstone, low angle cross bedding.	t = 290 - 775 cm l = 1 - 5 km	GR = 12 - 58 API DT = 167 - 397 µsm^{-1} NPHI = 0.05 - 0.595 v/v RHOB = 1612 - 2705 gcm-1	Proximal mouth bar
D	D1	Fining upward coarse to fine grained sandstone. Stacked fining upward beds with rare coarse grained stringers.	t = 740 - 820 cm l = 1 - 2 km	GR = 8 - 134 API DT = 235 - 335 µsm^{-1} NPHI = 0.14 - 0.46 v/v RHOB = 2284 - 2570 gcm-1	Tidal influenced fluvial channel fill sandstone
	D2	Fining upward coarse to medium grained sandstone. Carbonaceous laminae and fragments. Sharp and cohessive contact at base of bed.	t = 580 cm l = < 2 km	GR = 9 - 34 API DT = 241 - 297 µsm^{-1} NPHI = 0.14 - 0.289 v/v RHOB = 2168 - 2447 gcm-1	fluvial channel fill sandstone
E	E1	Coal and carbonaceous shale. Basal contact typically parallel, although maybe undulose.	t = 30 - 520 cm l = 6 - 19.6 km	GR = 8 - 56 API DT = 313 - 427 µsm^{-1} NPHI = 0.24 - 0.529 v/v RHOB = 1930 - 2225 gcm-1	Coal
	E2	Alternating dark grey mudstone/claystone and siltstone to very fine grained sandstone. Wavy to non-parallel lamination.	t = 60 cm l = < 2 km	GR = 32 - 60 API DT = 358 - 415 µsm^{-1} NPHI = 0.43 - 0.49 v/v RHOB = 1994 - 2148 gcm-1	Coastal plain fines
F	F	Mudstone with rare siltstone beds. Parallel lamination, soft sediment deformation developed locally on top of beds.	t = section tot completely penetrated l = 1.7 - 36.7 km	GR = 4 - 134 API DT = 187 - 450 µsm^{-1} NPHI = 0.114 - 0.618 v/v RHOB = 1730 - 2925 gcm-1	Open marine shale

Table 2. Input parameters ~~applied in running the~~for forward stratigraphic simulations in GPM™

For
Bo

Initial Conditions- GPM Input Parameters

GPM Scenarios (GS)	Simulation Duration	Sediment Type Proportion (%)				Avg. Water Velocity	Avg. Sediment Velocity	Erodibility	Diffusion Coefficient	Avg. Sea Level	Turbidite Event Interval	Steady Flow Iteration	Sediment Movement
	(Ma– 0a) Years	Sand (Coarse)	Sand (Fine)	Silt	Clay	(m/a)	(m/a)			Interval (m)	(/years)	(/hrs)	Coefficient
S1	0.02 – 0	25	25	25	25	0.11	0.03	0.35	0.11	30	2500	10	0.001
S2	0.25 – 0	25	25	25	25	0.15	0.03	0.45	0.15	70	1000	15	0.012
S3	0.5 – 0	25	25	25	25	0.11	0.02	0.55	0.11	120	1000	20	0.012
S4	0.7 – 0.05	25	25	25	25	0.08	0.02	0.35	0.08	100	500	25	0.0011
S5	1.5 – 0	15	35	30	20	0.15	0.04	0.50	0.15	80	5000	20	0.001
S6	3.0 – 0	50	25	15	10	0.13	0.04	0.50	0.13	70	5000	30	0.0012
S7	3.5 – 0	50	25	15	10	0.11	0.04	0.50	0.11	70	10000	15	0.001
S8	4.0 – 0	50	25	15	10	0.13	0.04	0.50	0.13	90	5000	20	0.0015
S9	4.5 – 0	15	45	25	15	0.1	0.02	0.45	0.1	50	10000	30	0.0012
S10	5.0 – 0	15	45	25	15	0.12	0.02	0.45	0.12	55	10000	35	0.0013
S11	5.5 - 0	15	45	25	15	0.12	0.02	0.45	0.12	40	5000	40	0.0013
S12	6.0 – 0	15	45	25	15	0.1	0.02	0.45	0.1	60	10000	35	0.0011
S13	6.5 – 0	10	25	55	10	0.13	0.03	0.48	0.13	100	20000	50	0.0010
S14	7.0 – 0	10	25	55	10	0.16	0.03	0.48	0.16	40	20000	45	0.0011
S15	7.5 – 0	10	25	55	10	0.13	0.03	0.48	0.13	40	20000	40	0.0012
S16	8.0 – 0	10	25	55	10	0.15	0.03	0.48	0.15	30	10000	30	0.0010
S17	8.5 – 0	10	25	45	20	0.14	0.02	0.45	0.14	50	50000	50	0.0010
S18	9.0 – 0	30	30	18	22	0.13	0.02	0.52	0.13	60	25000	35	0.0012
S19	9.5 – 0	30	40	12	18	0.12	0.02	0.55	0.12	55	25000	20	0.0013
S20	10.0 - 0	30	42	18	10	0.11	0.01	0.40	0.11	50	5000	15	0.0011

Sediment Property

Sediment Type	Diameter	Density	Initial Porosity	Initial Permeability	Compacted Porosity	Compaction	Compacted Permeability	Erodibility
Coarse Grained Sand	1.0 mm	2.70 g/cm^3	0.21 m^3/m^3	500 mD	0.25 m^3/m^3	5000 KPa	50 mD	0.6
Fine Grained Sand	0.1 mm	2.70 g/cm^3	0.3 m^3/m^3	100 mD	0.15 m^3/m^3	2500 KPa	5 mD	0.45
Silt	0.01 mm	2.65 g/cm^3	0.38 m^3/m^3	50 mD	0.12 m^3/m^3	1200 KPa	2 mD	0.3
Clay	0.001 mm	2.65 g/cm^3	0.48 m^3/m^3	5 mD	0.05 m^3/m^3	500 KPa	0.1 mD	0.15

		Initial Conditions- GPM Input Parameters												
		Simulation Duration	Sediment Type Proportion (%)				Avg. Water Velocity	Avg. Sediment Velocity	Erodibility	Diffusion Coefficient	Avg. Sea Level	Turbidite Event Interval	Steady Flow Iteration	Sediment Movement
GPM Scenarios (GS)		(Ma– 0a) Years	Sand (Coarse)	Sand (Fine)	Silt	Clay	(m/a)	(m/a)			Interval (m)	(/years)	(/hrs)	Coefficient
	S1	0.02 – 0	25	25	25	25	0.11	0.03	0.35	0.11	30	2500	10	0.001
	S2	0.25 – 0	25	25	25	25	0.15	0.03	0.45	0.15	70	1000	15	0.012
	S3	0.5 – 0	25	25	25	25	0.11	0.02	0.55	0.11	120	1000	20	0.012
	S4	0.7 – 0.05	25	25	25	25	0.08	0.02	0.35	0.08	100	500	25	0.0011
	S5	1.5 – 0	15	35	30	20	0.15	0.04	0.50	0.15	80	5000	20	0.001
	S6	3.0 – 0	50	25	15	10	0.13	0.04	0.50	0.13	70	5000	30	0.0012
	S7	3.5 – 0	50	25	15	10	0.11	0.04	0.50	0.11	70	10000	15	0.001
	S8	4.0 – 0	50	25	15	10	0.13	0.04	0.50	0.13	90	5000	20	0.0015
	S9	4.5 – 0	15	45	25	15	0.1	0.02	0.45	0.1	50	10000	30	0.0012
	S10	5.0 – 0	15	45	25	15	0.12	0.02	0.45	0.12	55	10000	35	0.0013
	S11	5.5 - 0	15	45	25	15	0.12	0.02	0.45	0.12	40	5000	40	0.0013
	S12	6.0 – 0	15	45	25	15	0.1	0.02	0.45	0.1	60	10000	35	0.0011
	S13	6.5 – 0	10	25	55	10	0.13	0.03	0.48	0.13	100	20000	50	0.0010
	S14	7.0 – 0	10	25	55	10	0.16	0.03	0.48	0.16	40	20000	45	0.0011
	S15	7.5 – 0	10	25	55	10	0.13	0.03	0.48	0.13	40	20000	40	0.0012
	S16	8.0 – 0	10	25	55	10	0.15	0.03	0.48	0.15	30	10000	30	0.0010
	S17	8.5 – 0	10	25	45	20	0.14	0.02	0.45	0.14	50	50000	50	0.0010
	S18	9.0 – 0	30	30	18	22	0.13	0.02	0.52	0.13	60	25000	35	0.0012
	S19	9.5 – 0	30	40	12	18	0.12	0.02	0.55	0.12	55	25000	20	0.0013
	S20	10.0 - 0	30	42	18	10	0.11	0.01	0.40	0.11	50	5000	15	0.0011

	Sediment Property								
	Sediment Type	**Diameter**	**Density**	**Initial Porosity**	**Initial Permeability**	**Compacted Porosity**	**Compaction**	**Compacted Permeability**	**Erodibility**
	Coarse Grained Sand	1.0 mm	2.70 g/cm^3	0.21 m^3/m^3	500 mD	0.25 m^3/m^3	5000 KPa	50 mD	0.6
	Fine Grained Sand	0.1 mm	2.70 g/cm^3	0.3 m^3/m^3	100 mD	0.15 m^3/m^3	2500 KPa	5 mD	0.45
	Silt	0.01 mm	2.65 g/cm^3	0.38 m^3/m^3	50 mD	0.12 m^3/m^3	1200 KPa	2 mD	0.3
	Clay	0.001 mm	2.65 g/cm^3	0.48 m^3/m^3	5 mD	0.05 m^3/m^3	500 KPa	0.1 mD	0.15

Table 3. Lithofacies classification in the forward stratigraphic model~~; showing the command used~~ in the property calculator tool in Petrel^{TM}.

Lithofacies Classification		
Facies Code	**Lithofacies**	**Command Used in Petrel's Property Calculator**
0	Marine Shale	If(Sand_fine>=0.19 And Sand_fine<=0.21 Or Silt>=0.19 And Silt<=0.2 Or Clay>=0.2 And Clay<=0.21 Or Depth_of_deposition>=-82 And Depth_of_deposition<=-78)
1	Muddy Shallow Bay Fill	If(Sand_fine>=0.36 And Sand_fine<=0.38 Or Silt>=0.18 And Silt<=0.2 Or Clay>0.18 And Clay<=0.19 Or Depth_of_deposition>=-30 And Depth_of_deposition<=-20)
2	Sandy Shallow Bay Fill	If(Sand_coarse>=0.65 And Sand_coarse<=0.73 Or Sand_fine>=0.18 And Sand_fine<=0.22 Or Silt>=0.18 And Silt<=0.2 Or Clay>=0.17 And Clay<=0.18 Or Depth_of_deposition>=-3 And Depth_of_deposition<=0)
3	Channel Fill Sandstone	If(Sand_coarse>=0.5 And Sand_coarse<=0.68 Or Sand_fine>=0.23 And Sand_fine<=0.25 Or Silt>=0.17 And Silt<=0.18 Or Depth_of_deposition>=0 And Depth_of_deposition<=2)
4	Lower Shoreface Units	If(Sand_coarse>=0.19 And Sand_coarse<=0.31 Or Sand_fine>=0.19 And Sand_fine<=0.24 Or Silt>=0.4 And Silt<=0.48 Or Clay>=0.19 And Clay<=0.31 Or Depth_of_deposition>=-83 And Depth_of_deposition<=50)
5	Middle Shoreface Units	If(Sand_coarse>=0.32 And Sand_coarse<=0.53 Or Sand_fine>=0.25 And Sand_fine<=0.32 Or Silt>=0.26 And Silt<=0.32 Or Clay>=0.19 And Clay<=0.21 Or Depth_of_deposition>=-38 And Depth_of_deposition<=-12)
6	Upper Shoreface Units	If(Sand_coarse>=0.53 And Sand_coarse<=0.72 Or Sand_fine>=0.28 And Sand_fine<=0.33 Or Silt>=0.16 And Silt<=0.21 Or Depth_of_deposition>=-10 And Depth_of_deposition<=6)
7	Distal Mouth Bar Units	If(Sand_fine>=0.23 And Sand_fine<=0.27 Or Silt>=0.38 And Silt<=0.43 Or Clay>=0.19 And Clay<=0.21 Or Depth_of_deposition>=-95 And Depth_of_deposition<=-80)
8	Proximal Mouth Bar Units	If(Sand_coarse>=0.53 And Sand_coarse<=0.71 Or Sand_fine>=0.27 And Sand_fine<=0.32 Or Silt>=0.16 And Silt<=0.21 Or Clay>=0.06 And Clay<=0.07 Or Depth_of_deposition>=-30 And Depth_of_deposition<=-27)
9	Tide Influenced Sandstones	If(Sand_coarse>=0.53 And Sand_coarse<=0.71 Or Sand_fine>=0.26 And Sand_fine<=0.31 Or Silt>=0.35 And Silt<=0.41 Or Depth_of_deposition>=-5 And Depth_of_deposition<=1)
10	Fluvial Channel Sandstones	If(Sand_coarse>=0.54 And Sand_coarse<=0.56 Or Sand_fine>=0.27 And Sand_fine<=0.29 Or Silt>=0.19 And Silt<=0.21 Or Depth_of_deposition>=-2 And Depth_of_deposition<=2)
11	Coal	Estimated as background attribute
12	Coastal plain fines	If(Silt>=0.31 And Silt<=0.43 Or Clay>=0.31 And Clay<=0.35 Or Depositional_depth>=-100 And Depositional_depth<=-40)
13	Marine Mudstone	If(Sand_fine>=0.36 And Sand_fine<=0.38 Or Silt>=0.4 And Silt<=0.52 Or Clay>=0.45 And Clay<=0.78 Or Depth_of_deposition>=-105 And Depth_of_deposition<=-90)

Lithofacies Classification		
Facies Code	**Lithofacies**	**Command Used in Petrel's Property Calculator**
0	Marine Shale	If(Sand_fine>=0.19 And Sand_fine<=0.21 Or Silt>=0.19 And Silt<=0.2 Or Clay>=0.2 And Clay<=0.21 Or Depth_of_deposition>=-82 And Depth_of_deposition<=-78)
1	Muddy Shallow Bay Fill	If(Sand_fine>=0.36 And Sand_fine<=0.38 Or Silt>=0.18 And Silt<=0.2 Or Clay>0.18 And Clay<=0.19 Or Depth_of_deposition>=-30 And Depth_of_deposition<=-20)
2	Sandy Shallow Bay Fill	If(Sand_coarse>=0.65 And Sand_coarse<=0.73 Or Sand_fine>=0.18 And Sand_fine<=0.22 Or Silt>=0.18 And Silt<=0.2 Or Clay>=0.17 And Clay<=0.18 Or Depth_of_deposition>=-3 And Depth_of_deposition<=0)
3	Channel Fill Sandstone	If(Sand_coarse>=0.5 And Sand_coarse<=0.68 Or Sand_fine>=0.23 And Sand_fine<=0.25 Or Silt>=0.17 And Silt<=0.18 Or Depth_of_deposition>=0 And Depth_of_deposition<=2)
4	Lower Shoreface Units	If(Sand_coarse>=0.19 And Sand_coarse<=0.31 Or Sand_fine>=0.19 And Sand_fine<=0.24 Or Silt>=0.4 And Silt<=0.48 Or Clay>=0.19 And Clay<=0.31 Or Depth_of_deposition>=-83 And Depth_of_deposition<=50)
5	Middle Shoreface Units	If(Sand_coarse>=0.32 And Sand_coarse<=0.53 Or Sand_fine>=0.25 And Sand_fine<=0.32 Or Silt>=0.26 And Silt<=0.32 Or Clay>=0.19 And Clay<=0.21 Or Depth_of_deposition>=-38 And Depth_of_deposition<=-12)
6	Upper Shoreface Units	If(Sand_coarse>=0.53 And Sand_coarse<=0.72 Or Sand_fine>=0.28 And Sand_fine<=0.33 Or Silt>=0.16 And Silt<=0.21 Or Depth_of_deposition>=-10 And Depth_of_deposition<=6)
7	Distal Mouth Bar Units	If(Sand_fine>=0.23 And Sand_fine<=0.27 Or Silt>=0.38 And Silt<=0.43 Or Clay>=0.19 And Clay<=0.21 Or Depth_of_deposition>=-95 And Depth_of_deposition<=-80)
8	Proximal Mouth Bar Units	If(Sand_coarse>=0.53 And Sand_coarse<=0.71 Or Sand_fine>=0.27 And Sand_fine<=0.32 Or Silt>=0.16 And Silt<=0.21 Or Clay>=0.06 And Clay<=0.07 Or Depth_of_deposition>=-30 And Depth_of_deposition<=-27)
9	Tide Influenced Sandstones	If(Sand_coarse>=0.53 And Sand_coarse<=0.71 Or Sand_fine>=0.26 And Sand_fine<=0.31 Or Silt>=0.35 And Silt<=0.41 Or Depth_of_deposition>=-5 And Depth_of_deposition<=1)
10	Fluvial Channel Sandstones	If(Sand_coarse>=0.54 And Sand_coarse<=0.56 Or Sand_fine>=0.27 And Sand_fine<=0.29 Or Silt>=0.19 And Silt<=0.21 Or Depth_of_deposition>=-2 And Depth_of_deposition<=2)
11	Coal	Estimated as background attribute
12	Coastal plain fines	If(Silt>=0.31 And Silt<=0.43 Or Clay>=0.31 And Clay<=0.35 Or Depositional_depth>=-100 And Depositional_depth<=-40)
13	Marine Mudstone	If(Sand_fine>=0.36 And Sand_fine<=0.38 Or Silt>=0.4 And Silt<=0.52 Or Clay>=0.45 And Clay<=0.78 Or Depth_of_deposition>=-105 And Depth_of_deposition<=-90)

Table 4. Porosity and Permeability ~~estimate in identified~~ estimates of lithofacies packages in the model area.

Code	Lithofacies	Average NPHI	Density Porosity	Estimated Porosity	KLOGH (mD)
0	Marine Shale	0.17 - 0.45	0.1	0.08 - 0.11	10.02 - 16.1
1	Muddy Shallow Bay Fill	0.17 - 0.42	0.1	0.08 - 0.13	23.85 - 102.3
2	Sandy Shallow Bay Fill	0.07 - 0.52	0.25	0.16 - 0.25	100.0 - 398.7
3	Channel Fill Sandstone	0.04 - 0.15	0.30	0.18 - 0.22	400.01 - 889.7
4	Distal Lower Shoreface	0.04 - 0.19	0.29	0.1 - 0.23	120.5 - 170.3
5	Proximal Shoreface	0.05 - 0.17	0.31	0.17 - 0.24	80.2 - 412.5
6	Upper Shoreface Units	0.09 - 0.11	0.28	0.21 - 0.26	650.2 - 1023.7
7	Distal Mouth Bar Units	0.08 - 0.17	0.27	0.09 - 0.17	170.5 - 223.1
8	Proximal Mouth Bar	0.05 - 0.59	0.12	0.19 - 0.21	130.5 - 314.3
9	Tide Influenced SS	0.14 - 0.46	0.26	0.15 - 0.20	220.0 - 512.6
10	Fluvial Sandstones	0.14 - 0.29	0.21	0.19 - 0.21	180.5 - 691.8
11	Coal	0.24 - 0.53	0.05	0.001	0.001
12	Coastal Plain Fines	0.43 - 0.49	0.06	0.04 - 0.12	5.2 - 34.6
13	Marine Mudstone	0.16 - 0.42	0.1	0.08 - 0.10	6.0 - 15.2

Code	Lithofacies	Avg. NPHI	Density Porosity	Estimated Porosity	KLOGH (mD)
0	Marine Shale	0.17 - 0.45	0.1	0.08 - 0.11	10.02 - 16.1
1	Muddy Shallow Bay Fill	0.17 - 0.42	0.1	0.08 - 0.13	23.85 - 102.3
2	Sandy Shallow Bay Fill	0.07 - 0.52	0.25	0.16 - 0.25	100.0 - 398.7
3	Channel Fill Sandstone	0.04 - 0.15	0.3	0.18 - 0.22	400.01 - 889.7
4	Distal Lower Shoreface	0.04 - 0.19	0.29	0.1 - 0.23	120.5 - 170.3
5	Proximal Shoreface	0.05 - 0.17	0.31	0.17 - 0.24	80.2 - 412.5
6	Upper Shoreface	0.09 - 0.11	0.28	0.21 - 0.26	650.2 - 1023.7
7	Distal Mouth Bar	0.08 - 0.17	0.27	0.09 - 0.17	170.5 - 223.1
8	Proximal Mouth Bar	0.05 - 0.59	0.12	0.19 - 0.21	130.5 - 314.3
9	Tidal Influenced Sandstone	0.14 - 0.46	0.26	0.15 - 0.20	220.0 - 512.6
10	Fluvial Sandstones	0.14 - 0.29	0.21	0.19 - 0.21	180.5 - 691.8
11	Coal	0.24 - 0.53	0.05	0.001	0.001
12	Coastal Plain Fines	0.43 - 0.49	0.06	0.04 - 0.12	5.2 - 34.6
13	Marine Mudstone	0.16 - 0.42	0.1	0.08 - 0.10	6.0 - 15.2

Table 5. ~~Comparison~~A comparison of a) porosity, and b) permeability estimates from selected intervals in the original ~~petrophysical model~~porosity/permeability models and forward modeling-based porosity and permeability models.

a. Validation Well Position 1							
	Porosity: GPM-Based Model					**Porosity: Original Model**	
	Depth (m)						
Models	5 m	10 m	15 m	25 m	35 m	**Depth (m)**	**Average Porosity**
R14	0.22	0.24	0.16	0.22	0.16	5	0.2
R20	0.16	0.19	0.26	0.18	0.15	10	0.25
R26	0.18	0.17	0.23	0.16	0.19	15	0.27
R36	0.22	0.21	0.19	0.22	0.21	25	0.16
R45	0.25	0.2	0.23	0.22	0.15	35	0.13
R49	0.21	0.17	0.22	0.17	0.18		
Validation Well Position 2							
	Porosity: GPM-Based Model					**Porosity: Original Model**	
	Depth (m)						
Models	5 m	10 m	15 m	25 m	35 m	**Depth (m)**	**Average Porosity**
R14	0.17	0.16	0.24	0.15	0.25	5	0.17
R20	0.21	0.22	0.2	0.21	0.23	10	0.21
R26	0.21	0.2	0.21	0.25	0.24	15	0.21
R36	0.2	0.22	0.21	0.21	0.19	25	0.17
R45	0.22	0.19	0.2	0.19	0.21	35	0.19
R49	0.26	0.24	0.23	0.16	0.21		

b. Validation Well Position 1							
	Permeability_Z (mD): GPM-Based Model					**Permeability_Z: Original Model**	
	Depth (m)						
Models	5 m	10 m	15 m	25 m	35 m	**Depth (m)**	**Average Perm_Z**
R14	163.95	312.38	69.84	310.16	508.2	5	352.74
R20	290.84	315.09	105.66	273.04	200.63	10	312.38
R26	375.92	203.81	166.23	189.92	348.12	15	201.08
R36	418.03	203.27	190.9	168.9	370.56	25	199.76
R45	337.6	412.67	199.66	156.71	305.92	35	508.2
R49	370.89	129.33	291.77	175.53	551.18		
Validation Well Position 2							
	Permeability_Z (mD): GPM-Based Model					**Permeability_Z: Original Model**	
	Depth (m)						
Models	5 m	10 m	15 m	25 m	35 m	**Depth (m)**	**Average Perm_Z**
R14	320.34	336.22	151.08	464.22	132.98	5	6.6
R20	122.66	209.15	161.3	230.58	208.48	10	883.6
R26	151.48	710.07	175.09	384.49	169.48	15	30.3
R36	184.74	344.99	157.08	420.15	136.14	25	496.99
R45	91.44	361.04	77.17	382.85	134.56	35	156.6
R49	134.01	721.73	137.42	636.48	290.06		

a. Validation Well Position 1					
	Depth (m)				
	5 m	10 m	15 m	25 m	35 m
Models	**Measured Porosity**				
Original Model	0.2	0.25	0.27	0.16	0.13
R14	0.22	0.24	0.16	0.22	0.16
R20	0.16	0.19	0.26	0.18	0.15
R26	0.18	0.17	0.23	0.16	0.19
R36	0.22	0.21	0.19	0.22	0.21
R45	0.25	0.2	0.23	0.22	0.15
R49	0.21	0.17	0.22	0.17	0.18
Validation Well Position 2					
	Depth (m)				
	5 m	10 m	15 m	25 m	35 m
Models	**Measured Porosity**				
Original Model	0.17	0.21	0.21	0.17	0.19
R14	0.17	0.16	0.24	0.15	0.25
R20	0.21	0.22	0.2	0.21	0.23
R26	0.21	0.2	0.21	0.25	0.24
R36	0.2	0.22	0.21	0.21	0.19
R45	0.22	0.19	0.2	0.19	0.21
R49	0.26	0.24	0.23	0.16	0.21

b. Validation Well Position 1					
	Depth (m)				
	5 m	10 m	15 m	25 m	35 m
Models	**Measured Permeability_Z (mD)**				
Original Model	352.74	312.38	201.08	199.76	508.2
R14	163.95	312.38	69.84	310.16	508.2
R20	290.84	315.09	105.66	273.04	200.63
R26	375.92	203.81	166.23	189.92	348.12
R36	418.03	203.27	190.9	168.9	370.56
R45	337.6	412.67	199.66	156.71	305.92
R49	370.89	129.33	291.77	175.53	551.18
Validation Well Position 2					
	Depth (m)				
	5 m	10 m	15 m	25 m	35 m
Models	**Measured Permeability_Z (mD)**				
Original Model	6.6	883.6	30.3	496.99	156.6
R14	320.34	336.22	151.08	464.22	132.98
R20	122.66	209.15	161.3	230.58	208.48
R26	151.48	710.07	175.09	384.49	169.48
R36	184.74	344.99	157.08	420.15	136.14
R45	91.44	361.04	77.17	382.85	134.56
R49	134.01	721.73	137.42	636.48	290.06